Petroleum Science 22 (2025) 90–109

Contents lists available at ScienceDirect

Petroleum Science

journal homepage: www.keaipublishing.com/en/journals/petroleum-science

Original Paper

Detailed oil-source correlation within the sequence and sedimentary framework in the Fushan Depression, Beibuwan Basin, South China Sea

Xin Wang [a, b, c], Mei-Jun Li [a, b, c, *], Yang Shi [d], Hao Guo [d], Bang Zeng [b, c], Xi He [a, b, c]

[a] Hainan Institute of China University of Petroleum (Beijing), Sanya, 572025, Hainan, China
[b] National Key Laboratory of Petroleum Resources and Engineering, China University of Petroleum (Beijing), Beijing, 102249, China
[c] College of Geosciences, China University of Petroleum (Beijing), Beijing, 102249, China
[d] Southern Oil Exploration and Development Company, PetroChina, Haikou, 570216, Hainan, China

ARTICLE INFO

Article history:
Received 27 March 2024
Received in revised form
11 June 2024
Accepted 18 August 2024
Available online 22 August 2024

Edited by Min Li

Keywords:
Oil-source correlation
Sequence stratigraphic framework
Biomarkers
Fushan depression
South China Sea

ABSTRACT

The Fushan Depression is one of the petroliferous depressions in the Beibuwan Basin, South China Sea. Previous studies have preliminarily explored the origin and source of crude oils in some areas of this depression. Nevertheless, no systematic investigations on the classification and origin of oils and hydrocarbon migration processes have been made for the entire petroleum system in this depression, which has significantly hindered the hydrocarbon exploration in the region. A total of 32 mudstone and 58 oil samples from the Fushan Depression were analyzed to definite the detailed oil-source correlation within the sequence and sedimentary framework. The organic matter of third member of Paleogene Liushagang Formation (Els_3) source rocks, both deltaic and lacustrine mudstone, are algal-dominated with high abundance of C_{23} tricyclic terpane and C_{30} 4-methylsteranes. The deltaic source rocks occurring in the first member (Els_1) and second member (Els_2) of the Paleogene Liushagang Formation are characterized by high abundance of C_{19+20} tricyclic terpane and oleanane, reflecting a more terrestrial plants contribution. While lacustrine source rocks of Els_1 and Els_2 display the reduced input of terrigenous organic matter with relatively low abundance of C_{19+20} tricyclic terpane and oleanane. Three types of oils were identified by their biomarker compositions in this study. Most of the oils discovered in the Huachang and Bailian Els_1 reservoir belong to group A and were derived from lacustrine source rocks of Els_1 and Els_2. Group B oils are found within the Els_1 and Els_2 reservoirs, showing a close relation to the deltaic source rocks of Els_1 and Els_2, respectively. Group C oils, occurring in the Els_3 reservoirs, have a good affinity with the Els_3 source rocks. The spatial distribution and accumulation of different groups of oils are mainly controlled by the sedimentary facies and specific structural conditions. The Els_2 reservoir in the Yong'an area belonging to Group B oil, are adjacent to the source kitchen and could be considered as the favorable exploration area in the future.

1. Introduction

Defining the crude oil geochemical characteristics and oil-source relationships is critical for determining hydrocarbon accumulation features in a petroleum system with complex structural and multiple sets of source rock (Hao et al., 2011; Huang et al., 2011; Schwangler et al., 2020). Biomarkers can reflect the organic matter source, depositional environment and maturity of source rocks and oils, and are widely applied to analyze the oil sources in sedimentary basins (Peters et al., 2005). The changes of sedimentary environment and organic matter input in different sedimentary periods lead to different biomarker assemblage characteristics (Bohacs et al., 2000; Peters et al., 2000; Li et al., 2018a; Lai et al., 2018; Zhu et al., 2022). Over the same period, the greater sedimentary facies variation in lacustrine basin also yields distinct biomarker compositions (Huang et al., 2017; Lu et al., 2022; Zeng et al., 2022). Considerable heterogeneity of source rocks may result in the

* Corresponding author. State Key Laboratory of Petroleum Resources and Engineering, China University of Petroleum (Beijing), Beijing, 102249, China.
E-mail address: meijunli@cup.edu.cn (M.-J. Li).

https://doi.org/10.1016/j.petsci.2024.08.005

generation of oils with diverse geochemical characteristics (Zeng et al., 2022). Detailed oil-source correlation within the sequence and sedimentary framework could provide a more practical model for petroleum system study (Xiao et al., 2019a; Lai et al., 2020).

The Beibuwan Basin, one of the most important petroliferous basins in the northern continental margin of the South China Sea, consists of a set of clastic Cenozoic strata (Huang et al., 2013). The Fushan Depression presents rich hydrocarbon abundance in the Beibuwan Basin, which experienced multistage fault activities, causing the oils widely accumulated in Paleogene formations (Wang et al., 2016; Gan et al., 2020). The Paleogene Liushagang Formation has been proved as potential source rocks for the oils in this region (Zeng et al., 2022). The Huachang Uplift in the central part divides the Fushan Depression into two sub-depressions, resulting in significant differences in sequences and tectonic styles (Ma et al., 2012). The geochemical characteristics of the Liushagang Formation are clearly clarified and those of the related oils are also revealed in the Bailian area, the eastern parts of the depression (Gan et al., 2020, 2023). The biomarker composition of the crude oils in the western area were also reported (Lu et al., 2016; Wang et al., 2022a). However, the correlation between the crude oils in the western and eastern area have yet to be elucidated, and systematic analysis of the origin and source of oils in the entire depression is still limited.

The distribution and accumulation of hydrocarbons are subject to the transfer zone and special double-layered tectonostratigraphic framework, as indicated by the established accumulation model (Li et al., 2007; Wang et al., 2016; Gan et al., 2020, 2023). Due to the presence of multiple sets of source rocks and the multistage petroleum charging, the accumulation pattern of certain area is not applicable to the entire Fushan Depression. The directions of hydrocarbon migration in Fushan Depression have been traced by geochemical parameters and the locations of potential source rocks have been predicted (Yang et al., 2016; Fang et al., 2017; Li et al., 2018b). A systematic and comprehensive analysis of the hydrocarbon accumulation model remains to be clarified.

In this work, we conducted a detailed geochemical analysis on the crude oils and source rocks of the entire Fushan Depression. The purposes of this study include (1) to evaluate the geochemical characteristics of crude oils, (2) to identify the oil-source relationship within the sequence and sedimentary framework, (3) to analyze the hydrocarbon migration and accumulation characteristics. Advancement of a comprehensive understanding of the oil source relationship and its distribution within the study area is of great importance, as it would improve an understanding of hydrocarbon accumulation and the accuracy of petroleum resource evaluation in the sag.

2. Geological setting

Fushan Depression is a typical rift subsidence lacustrine basin with multiphase structural superposition and diverse sediment types. It is bounded by the Lingao Fault to the west, the Changliu Fault to the east and the Anding Fault to the south, covering an area of 2920 km^2. The Bohou Fault, Meihua Fault and Lianhua Fault are important secondary faults, which divided the whole depression into several primary structural units, including the northern step fault zone, the Huangtong Sag, the transfer zone and the southern slope zone (Fig. 1). The transfer zone occurred in the central region results in different tectonic styles and sedimentary patterns between the western and eastern areas (Fig. 2) (Ma et al., 2012; Liu et al., 2015). The Liushagang Formation in the southern slope zone was divided into two sets of fault systems vertically, which is more apparent in the east area (Gan et al., 2020, 2023).

The Paleogene stratigraphic sequences consist of the Paleocene Changliu Formation (E*ch*), the Eocene Liushagang Formation (E*ls*) and the Oligocene Weizhou Formation (E*wz*) (Fig. 3). The Changliu Formation was mostly deposited as fluvial facies during the early rifting period. The Liushagang Formation is composed of fan delta, braided river delta and lacustrine sedimentary system, and the Weizhou Formation comprises the fluvial facies intercalated with shallow marine deposits. The Liushagang Formation is the main source and oil-bearing bed, which is sub-divided into three members, i.e. Els_3, Els_2 and Els_1, corresponding to the SQls3, SQls2 and SQls1 sequences, respectively (Liu et al., 2012; Ma et al., 2012). Each sequence is further divided into two system tracts—the expanding system tract (EST) and the regressive system tract (RST)—by the maximum flooding surface (mfs) (Gan et al., 2020; Zeng et al., 2022). The sedimentary evolution of the Fushan Depression is influenced by boundary faults, forming a multi-directional provenance system (Zeng et al., 2022). Sediment accumulation is supplied through braided river delta mainly from the southern margin and fan delta from the northwestern and northeastern margin. The Els_2 was the most substantial lacustrine transgression period of the lacustrine basin, forming a set of sublacustrine fans in the lowstand system tract (Liu et al., 2014; Li et al., 2017).

The study area has been under exploration for more than sixty years, with a yield of 400,000 tons per year (Gan et al., 2020; Wang et al., 2022a). Huachang Uplift, developed above the transfer zone in the central region, was the main exploration area in the early stage. The Els_3 is the prime stratum for condensate oil exploration in the Huachang and Bailian area. With the advance of hydrocarbon exploration, the exploration focus shifted to the western area, resulting in the discovery of Yong'an, Chaoyang, Hongguang and Meitai oil fields (Fig. 1).

3. Samples and methods

3.1. Samples

A total of 32 source rock samples were collected from the entire depression, including 18 samples from the delta facies and 14 from the lacustrine facies. The oil reservoirs in the Fushan depression laterally occurred in the east, west and central Huachang uplift (Fig. 1), and vertically in the strata of Els_3, Els_2, Els_1 and E*wz*. A sum of 58 crude oil samples were collected from different oil fields for systematic oil-source correlation. The core and oil samples geochemically analyzed using gas chromatography-mass spectrometry (GC-MS). The total organic carbon measurement and pyrolysis analysis were performed to identify the hydrocarbon generation potential of source rocks. Additionally, a total of 57 cuttings from M1, L15 and Y11 wells were sampled for vitrinite reflectance measurement.

3.2. Methods

Grinding the core sample to rock powder less than 80 mesh. Carbonates in rock samples were removed using hydrochloric acid, and the total organic carbon was then quantified on LECO CS-230 Carbon/Sulfur Analyzer. Rock-eval pyrolysis analysis was carried out with OGE-VI type pyrolyzer. A sample of 100 mg was weighed and heated to 600 °C to obtain the Rock-eval parameters.

The vitrinite reflectance (R_o%) was measured using a Leica Model MPV-SP microscopic photometer. The Petromod-1D software was applied to reconstruct the burial and thermal history, which was calibrated by the measured R_o (%). Data for modeling,

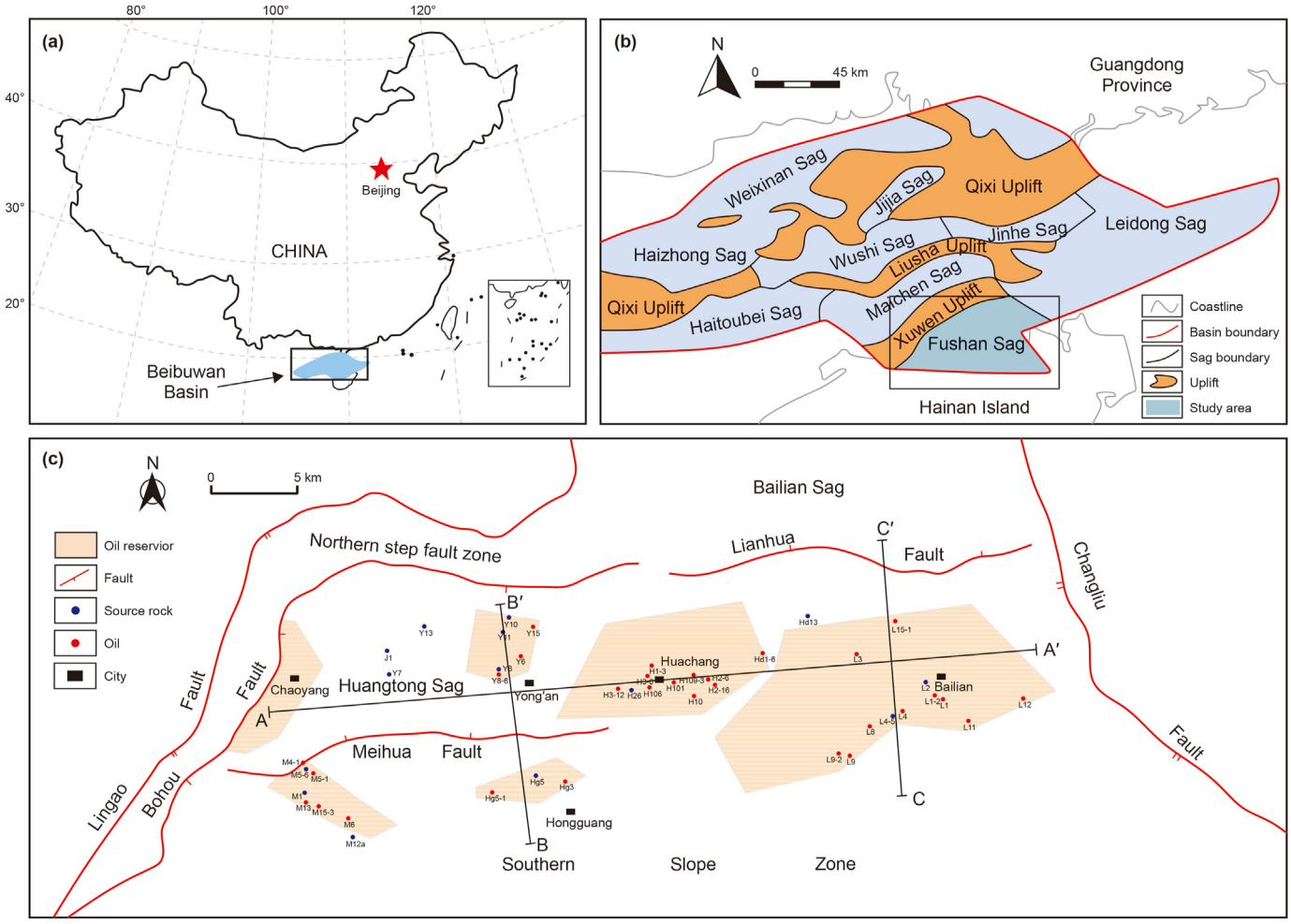

Fig. 1. Geological maps showing **(a)** the location of the Beibuwan Basin, **(b)** the structural divisions of the Beibuwan Basin, **(c)** the tectonic distribution units and sampling wells in the Fushan Depression (A − A′, B − B′ and C − C′ is the selected profile).

i.e., stratigraphic thickness, lithologies, erosion thickness, were provided by the Southern Oil Exploration and Development Company.

The rock powder was extracted for 24 h in the Soxhlet apparatus with 400 mL dichloromethane and methanol as the solvent (93:7, *v*:*v*). Asphaltenes were precipitated from the extracts by 50 mL of *n*-hexane. The remains were separated into saturated and aromatic hydrocarbons using alumina/silica gel columns, with 30 mL of *n*-hexane and dichloromethane: *n*-hexane (2:1, *v*:*v*) as eluents, respectively.

The saturated fraction was performed on Agilent 6890 GC-Agilent 5975i mass spectrometry system with an HP-5MS fused silica capillary column (30 m × 0.25 mm × 0.25 μm). The initial GC oven temperature was maintained at 50 °C for 1 min, then increased at a rate of 20 °C/min up to 120 °C, further increased at 3 °C/min to 310 °C, then finally held at 310 °C for 25 min. GC-MS analysis of aromatic hydrocarbon fractions was analyzed using an Agilent 7890B GC-Agilent 5977A MS system with an HP-5MS fused silica capillary column (60 m × 0.25 mm × 0.25 μm). The GC heating procedure as follows: 80 °C as the initial temperature for 1 min, then ramped up to 310 °C at a rate of 3 °C/min, and held at 310 °C for 20 min. Helium was the carrier gas for GC of the saturated and aromatic fractions. The chromatograph operated in electron impact (EI) mode, the ionization energy of the MS system was 70 eV, and the scanning range was *m/z* 50–600.

4. Results

4.1. Source rock classification

The geochemical characteristics of source rocks in the lacustrine basins show great lateral heterogeneity due to the variations of sedimentary facies (Zeng et al., 2022; Lai et al., 2020). Two type source rocks were generally distinguished in the continental lacustrine basins: deltaic source rocks and lacustrine source rocks (Er et al., 2015; Fu et al., 2018; Lu et al., 2022). The deltaic source rocks are formed near the margin of basin with more terrigenous organic matter input. While the lacustrine source rocks deposited in the center of lacustrine basin are contributed by more aquatic organism (Yuan et al., 2022). Gray and dark-gray mudstones from the delta-lacustrine sedimentary system are widely present throughout the Fushan Depression (Gan et al., 2020, 2023). In terms of the sedimentary facies, the Liushagang Formation mudstones can be divided into delta plain mudstones, delta front mudstones, shallow lake mudstones, semi-deep lake mudstones, fan delta front mudstones, turbidite fan mudstones (Zeng et al., 2022). Turbidite fan is mainly formed through the slumping of delta front. The organic matter sources of turbidite fan and delta front are similar, while the preservation conditions may be different (Liu et al., 2003, 2014; Wang et al., 2014; Li et al., 2022). Turbidite fans are generally thought to be preserved in the deep-lake reducing environment,

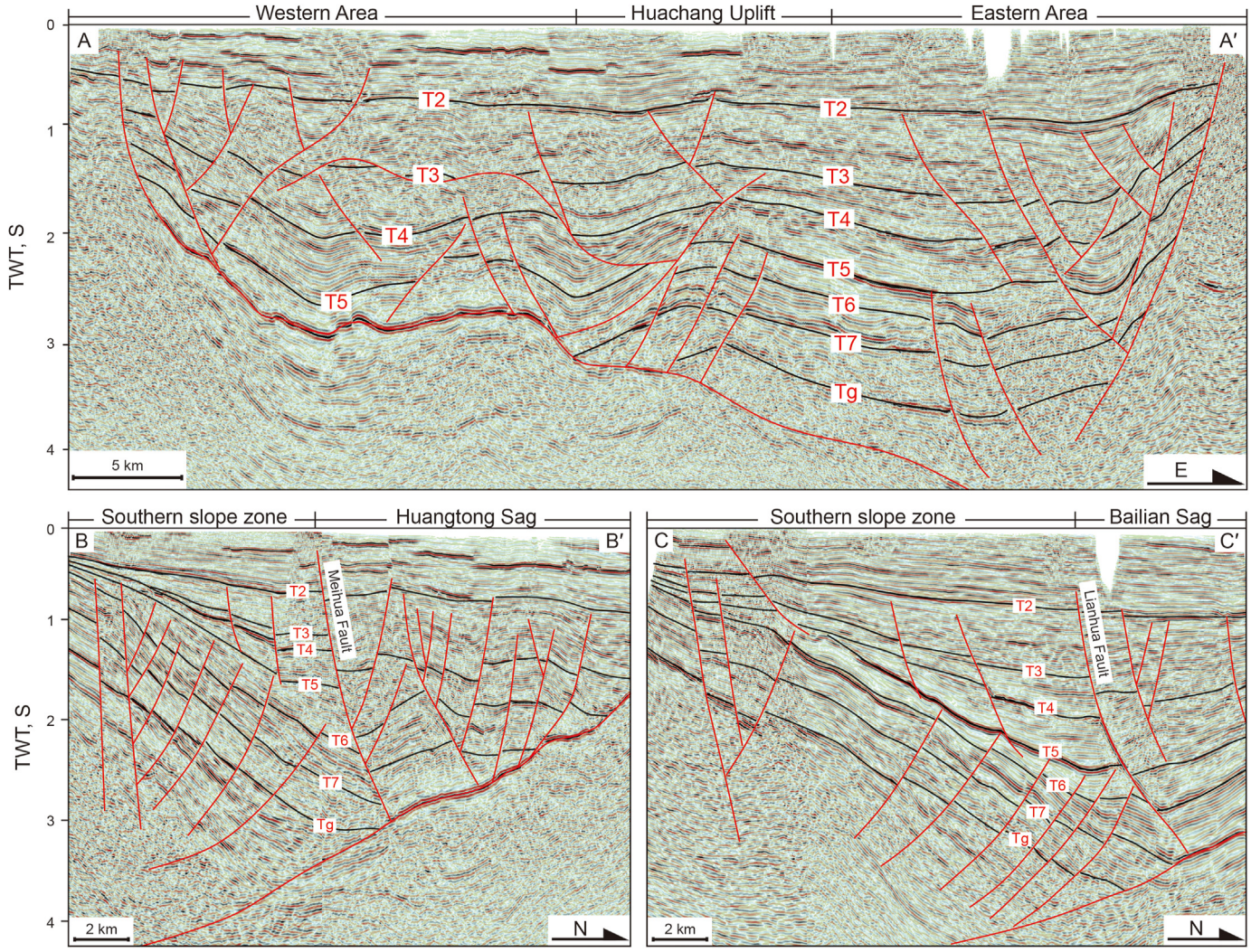

Fig. 2. Interpreted seismic section AA' (W-E direction) BB' (S–N direction in western area) CC'(S–N direction in eastern area) showing the tectonic style of Fushan Depression. The location of the section is shown in Fig. 1.

whereas delta fronts are in relative oxidizing condition. Source rocks in the Fushan Depression are deposited in a mildly oxidizing shallow lacustrine environment (Gan et al., 2020). In this study, we defined the source rocks both from turbidite fan and delta front as "source rock from delta".

Considering the depositional characteristics of the Fushan Depression, the Liushagang Formation source rocks were divided into lacustrine mudstones and deltaic mudstones. Mudstones from different sedimentary environments exhibit distinct well log responses and mudstone to stratum thickness ratios (M/S ratios) (Fig. 4). Lacustrine mudstones, deposited in a deep-water environment with abundant plankton and algal input, are characterized by thick and continuous gray-dark mudstones (Zhang et al., 2015; Lu et al., 2022). The M/S ratios are generally higher than 0.8 and the GR curves are low amplitude linear shapes. On the contrary, the mudstones in delta facies have more terrestrial plants input. Due to the strong hydrodynamic power, the deltaic mudstones are dominated by massive mudstones with sandstone and siltstone intervals, forming the thin and discontinuous source rocks (Er et al., 2015; Lu et al., 2022). The M/S ratios are estimated to be between 0.6 and 0.8 and the well logging of delta deposits exhibit bell and funnel-shaped GR curves.

4.2. Hydrocarbon generating potential of source rocks

4.2.1. Organic carbon content and organic matter type in source rocks

Mudstones from the Liushagang Formation are characterized by variable TOC contents, ranging from 0.58%–2.32% with an average of 1.38%. The hydrocarbon potential index (S_1+S_2) varies from 1.83 to 6.81 mg HC/g rock, indicating good source rocks in terms of the S_1+S_2 (mg HC/g rock) versus TOC (wt%) plot (Robison et al., 1999; Xiao et al., 2019b) (Fig. 5(a)). The hydrogen index (HI) is in the range of 139–360 mg HC/g TOC, corresponding to type II_1 and II_2 kerogen according to the hydrogen index (HI, mg HC/g TOC) versus T_{max} plot (Mukhopadhyay et al., 1995; Xiao et al., 2019b) (Fig. 5(b)). In addition, an average T_{max} of 445 °C, with a range of 434–456 °C, indicates that the Liushagang Formation source rocks have entered the oil generation window.

It is generally believed that source rocks are mostly present in shallow lake and medium-deep lake environment in the lacustrine basin, and the hydrocarbon generation potential of delta source rocks is generally overlooked (Zhao et al., 2016; Huang et al., 2017; Liang et al., 2018). Source rocks from the lacustrine facies usually displayed high TOC contents and favorable organic matter type (Er et al., 2015; Lu et al., 2022). While Lai et al. (2020) considered that

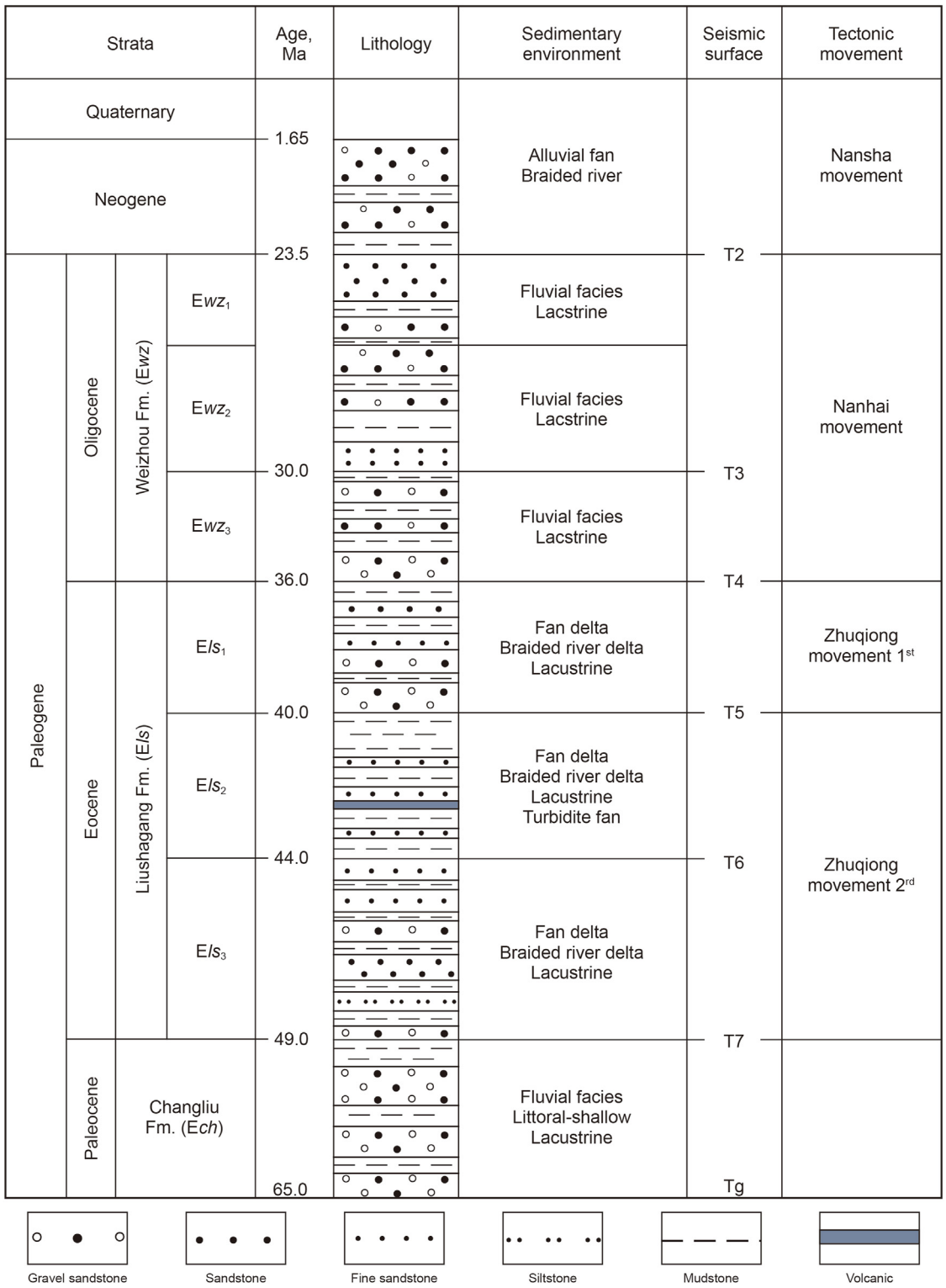

Fig. 3. Schematic stratigraphic column in the Fushan Depression.

prodeltaic mudstones have excellent hydrocarbon potential than the lacustrine mudstones in the North Yellow Sea Basin. No evident difference in hydrocarbon generation potential of source rocks among the sedimentary environments in the study area (Fig. 5), which may be attributed to the shallow water depth without strong reducing environment deposited during the sedimentary period of Liushagang Formation (Gan et al., 2020).

4.2.2. Organic matter maturity

Based on the measured vitrinite reflectance and the modeled thermal evolution history, the $E\ell s_3$ source rocks in the western area are in the low-mature to mature stage (Fig. 6(a)). While the thermal

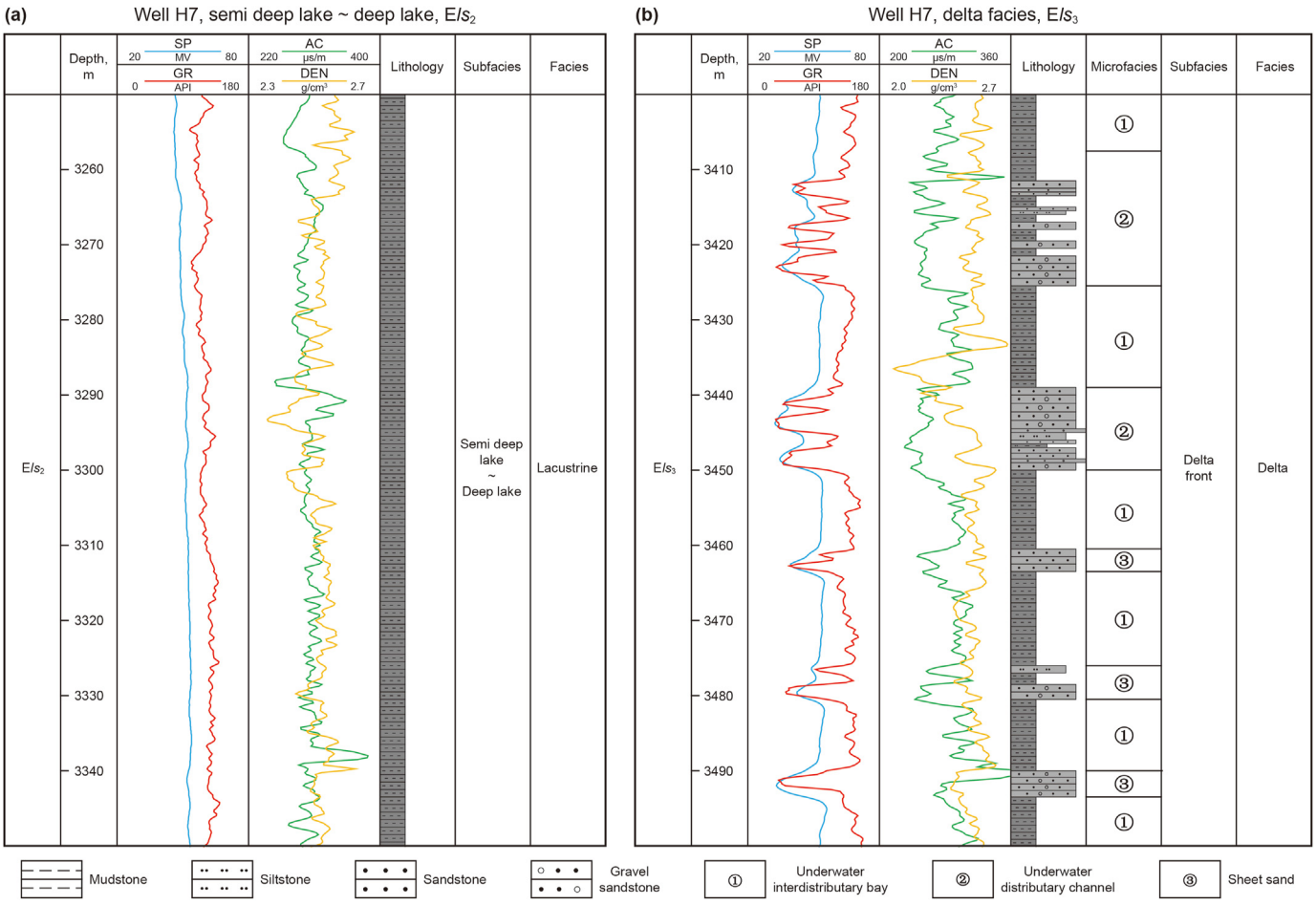

Fig. 4. Logging response characters of the Liushagang Formation source rocks from different sedimentary environments in the Fushan Depression.

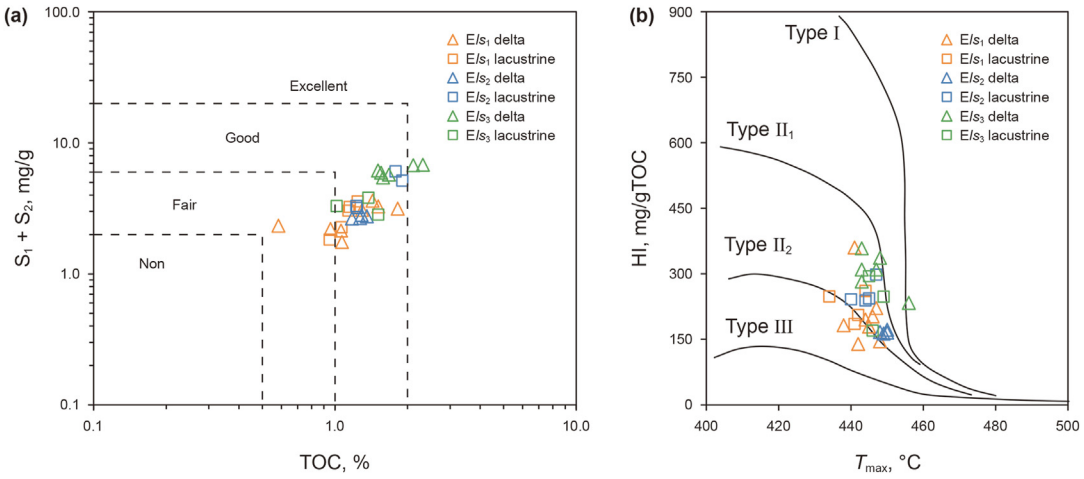

Fig. 5. Variation of **(a)** (S_1+S_2) with total organic carbon content (according to the standard SY/T 5735-2019) and **(b)** hydrogen index with T_{max} (after Bordenave et al. (1993)) for showing the hydrocarbon-generating potential and organic matter type of source rocks from the Fushan Depression, respectively.

maturity of Els_3 source rocks in the eastern area is higher than that of the western area with a mature stage currently (Fig. 6(b)). The selected well in the eastern area is located at the edge of the depression, and the maturity in the central basin might be higher. Two-dimensional thermal maturity evolution profile of the eastern area shows that the maximum buried depth of the Els_3 exceed 5000 m, and the Ro can reach 1.3%, which can also be confirmed by the thermal evolution simulation of the virtual well located in the center of the depression (Chen et al., 2014; Zeng et al., 2023).

The Els_2 source rocks in the eastern area have entered the mature stage, while the source rocks in the western area are still in the low-mature stage. The Els_1 and Els_2 source rocks in the

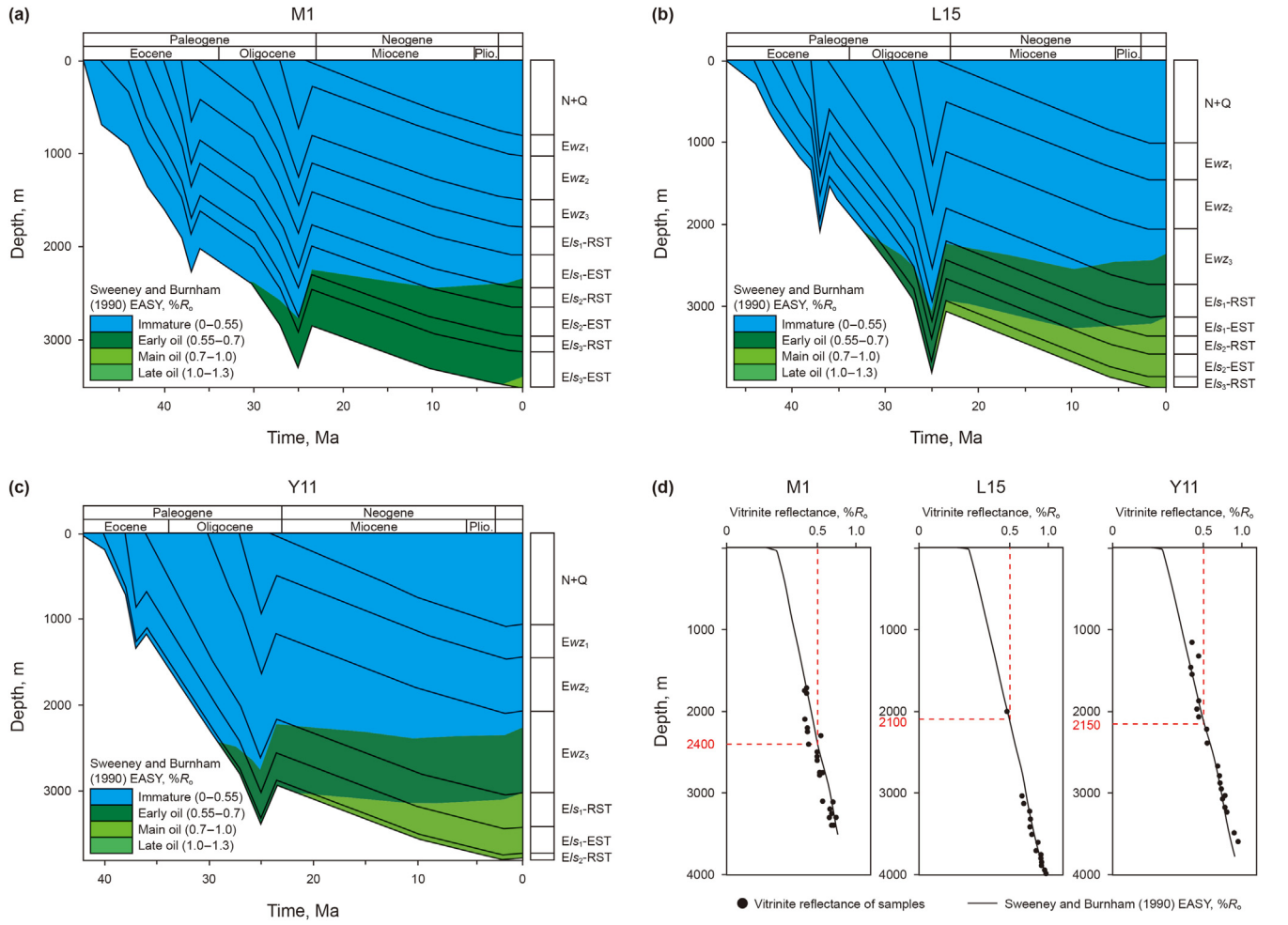

Fig. 6. Thermal evolution history of selected well in the Fushan Depression.

Huangtong Sag are in mature stage (Fig. 6(c)). The higher heat flow in the eastern area, influenced by the volcanic intrusion, lead to the shallower threshold of hydrocarbon generation compared to the western area (Fig. 6(d)) (Zeng et al., 2023). Volcanic intrusion in the eastern area may also result in the abnormal higher Ro value (Liu et al., 2017, 2021; Zeng et al., 2023).

4.3. Geochemical characteristics of source rocks

4.3.1. Distribution of normal-alkanes and isoprenoids

Normal-alkanes and isoprenoids are important biomarkers to identify the organic matter source, sedimentary environment and thermal maturity. The gas chromatograms of saturated hydrocarbons of most source rock samples show a bimodal distribution pattern (Fig. 7). Moreover, values of $\sum C_{22+}/\sum C_{21-}$ ratio range from 0.87 to 4.25 with an average of 1.78, reflecting a predominantly terrestrial organic matter input with subordinate aquatic organism input. The pristane to phytane ratios (Pr/Ph) range from 1.40 to 5.50, suggesting an oxic to suboxic depositional environment (Supplementary Table 1). According to the cross plot of Pr/nC_{17} versus Ph/nC_{18} (Fig. 8(a)), all samples were deposited in an oxidizing environment, as indicated by the low content of dibenzothiophene (DBT) (Fig. 8(b)).

4.3.2. Distribution of terpanes and hopanes

The relative abundance of tricyclic terpanes reflects the organic matter input and depositional environment, which have been commonly used in oil–source correlation studies (Zhang and Huang, 2005; Tao et al., 2015). C_{19}TT and C_{20}TT may be derived from diterpenoids, indicating the biogenic characteristics of terrestrial organisms, while C_{23}TT is dominant in source rocks from saline lacustrine and marine environments (Ekweozor and Strausz, 1983; Peters et al., 2005; Xiao et al., 2019c, 2024). Additionally, three unusual tetracyclic terpanes (designed as compounds Y_1, Z and Z_1) were also recognized in the source rock samples, which were determined to be C_{24}-des-A-oleanane, C_{24} des-A-ursane and C_{27} tetracyclic terpane by comparison of ion fragments and retention time with published literature (Samuel et al., 2010; Xiao et al., 2018; Wang et al., 2022b). The representative mass spectra and molecular structures of the three unusual tetracyclic terpanes after subtracting the background mass spectra are shown in Fig. 9. These unusual tetracyclic terpanes have been detected in the crude oils of the Fushan Depression (Xiao et al., 2018; Wang et al., 2022b), which have also been identified for the first time in the source rocks from the Liushagang Formation of the Fushan Depression. The high abundance of these biomarkers is probably related to the contribution of higher plant material in the organic matter (Chattopadhyay and Dutta, 2014; Samuel et al., 2010; Xiao et al., 2018).

The Els_1 and Els_2 source rocks from the delta facies are characterized by a predominance of C_{19}TT and C_{20}TT among the tricyclic terpanes series, with the C_{19+20}/C_{23}TT ratios ranging from 3.24 to

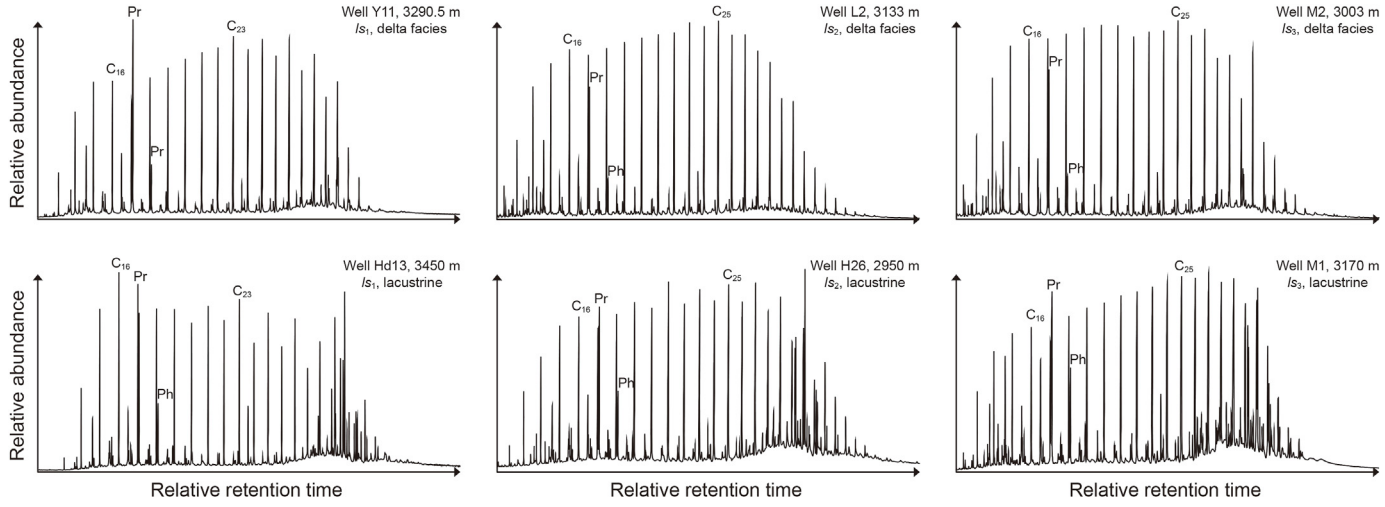

Fig. 7. Representative TIC of saturated hydrocarbon showing the distribution of normal alkanes and acyclic isoprenoids.

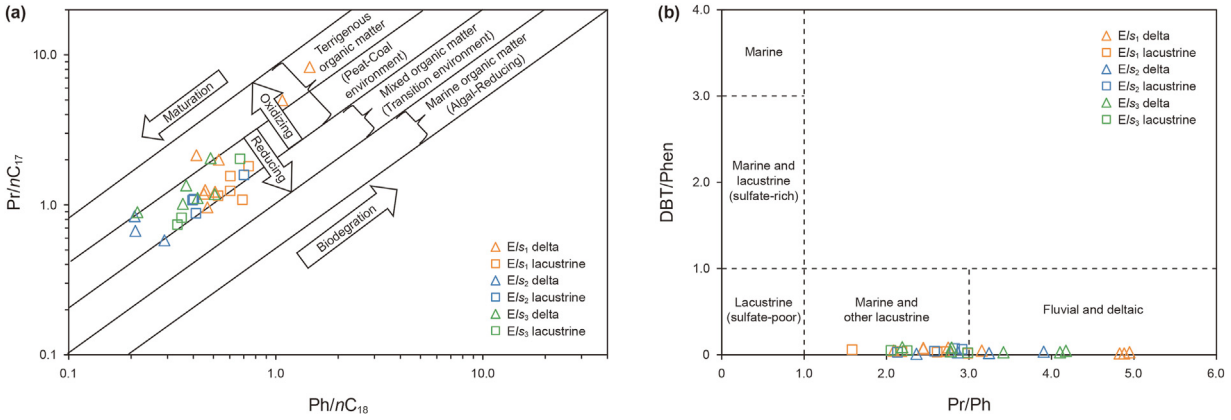

Fig. 8. Cross plots of Pr/nC_{17} vs. Ph/nC_{18} **(a)** (after Shanmugam (1985)) and DBT/Phen vs Pr/Ph **(b)** (after Hughes et al. (1995)) for showing the deposition conditions of source rocks from the Fushan Depression.

7.54 (average 4.97). While the C_{19+20}/C_{23}TT ratio for the lacustrine source rocks was only 0.93–2.14 (average 1.84) (Supplementary Table 1). Consistent with the abundant C_{19}TT and C_{20}TT, the relatively high concentrations of oleanane and unusual tetracyclic terpanes in the Els_1 and Els_2 deltaic source rocks indicate greater terrigenous high plant input (Figs. 10 and 12). The Els_1 and Els_2 lacustrine source rocks exhibit a relatively low abundance of C_{19+20} tricyclic terpane and oleanane, showing the less terrestrial plants input compared to the delta source rock (Figs. 11 and 12).

Most Els_3 source rocks, both from the delta and lacustrine, have a remarkably high abundance of C_{23}TT and low content of oleanane and unusual tetracyclic terpanes, indicating the dominated organic matter sourced from aquatic organisms (Figs. 10 and 11). The similar geochemical characteristics observed in different sedimentary facies of Els_3 source rocks may be attributed to the less terrestrial plants input during the Els_3 depositional period.

Gammacerane is a diagnostic biomarker for water column stratification (Moldowan et al., 1985; Sinninghe Damsté et al., 1995). Its abundance in all source rock samples is extremely low ($Ga/C_{30}H < 0.1$), which is commonly associated with a freshwater lacustrine depositional setting. The distribution of C_{31}–C_{35} hopanes can be used to evaluate redox conditions and depositional environment (Peters et al., 2005). Generally, a relatively high abundance of C_{35} hopane is related to the high-salinity lacustrine or strong-reducing marine conditions (Peters et al., 2005; Hao et al., 2011). The gradual decrease from C_{31} to C_{35} hopane series further implies the fresh lacustrine sedimentary environment (Figs. 10 and 11).

4.3.3. Distribution of steranes and methyl-triaromatic steroids

C_{27}–C_{29} regular steranes (C_{27}–C_{29}St) and C_{30} 4α-methylsteranes (C_{30} 4-Me St) were identified in *m/z* 217 mass chromatograms of saturated hydrocarbon fraction, which is commonly applied to analyze organic matter sources. The C_{27}–C_{28}–C_{29} regular sterane ternary diagram shows that the organic matter in these samples is mixed contribution of bacteria, algae, and terrigenous plant material (Fig. 13). C_{30} 4-Me St is considered to be derived from dinoflagellates or haptophyte microalgae (Wolff et al., 1986; Volkman et al., 1990), which are presented in the Els_3 source rocks at a considerable abundance with higher 4-Me/C_{29}St ratios (0.35–0.55). Whereas the relative abundances of C_{30} 4-Me St are very low in Els_1 and Els_2 source rocks, with 4-Me/C_{29}St ratios ranging from 0.14 to 0.25 (Figs. 10 and 11).

Methyl-triaromatic steroids were also identified in *m/z* 245 mass chromatograms of aromatic hydrocarbons. The triaromatic dinosteroids (dino-TAS, C_{29} 4α,23,24-trimethyltriaromatic steroids) are generally thought to be originate from dinoflagellates. The triaromatic dinosteroid index (TDSI = dino-TAS/dino-TAS+3-methyltriaromatic steroids+4-methyltriaromatic steroids) is an

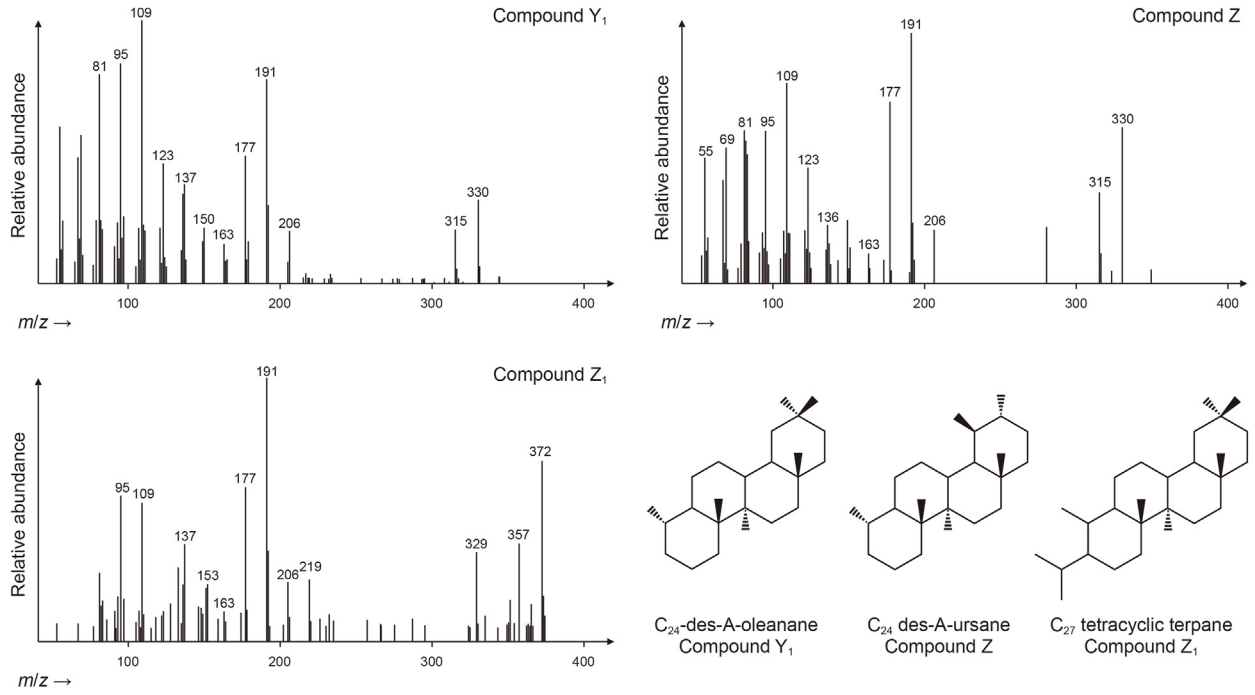

Fig. 9. Representative mass spectra of compounds Y_1, Z and Z_1, and molecular structures of compounds Y_1, Z and Z_1.

effective parameter for evaluating the organic matter inputs of source rocks (Wang et al., 2008; Chang et al., 2023). Lacustrine source rocks from E*ls*$_1$ and E*ls*$_2$ exhibit similar distributions of dino-TAS with TDSI exceed 0.43, corresponding to significant contributions from the dinoflagellates. However, the low abundances of dino-TAS in the E*ls*$_1$ and E*ls*$_2$ deltaic source rocks coincide with their low abundances of C_{30} 4-Me St, suggesting minor dinoflagellates contributions (Fig. 13). The E*ls*$_3$ source rocks from the eastern area have abundant dino-TAS (TDSI = 0.42–0.45), while the TDSI of source rocks from the western area are less than 0.32 (Fig. 13).

4.4. Geochemical characteristics of crude oil

4.4.1. Physical properties

In general, the crude oils in the Fushan Depression are dominated by light oil and condensate oil with the density below 0.85 g/cm^3. In comparison, the E*ls*$_2$ and E*ls*$_3$ oils from the eastern area, Huachang and Bailian area, have lower density of 0.76–0.82 g/cm^3. Whereas E*ls*$_3$ oils from Hongguang-Meitai area, in the western of Fushan Depression, has a normal density of 0.81–0.84 g/cm^3. Similar to the density, the E*ls*$_2$ and E*ls*$_3$ oils from the eastern area exhibit lower viscosity compared to those from the western area. All crude oil samples were characterized by relatively high saturated hydrocarbon contents with an average of 73.19%.

4.4.2. Biomarker compositions of the crude oil

The E*ls*$_1$ crude oils mainly distributed in Yong'an, Huachang and Bailian area. The oil samples from Yong'an area were found to contain evident distribution of C_{19+20} tricyclic terpane and oleanane, indicating the terrigenous organic matter input to the corresponding source rocks (Fig. 14). Furthermore, the low abundance of C_{30} 4-Me St and dino-TAS in the Yong'an oils reveal the minor contributions from dinoflagellates (Fig. 14). Crude oils from the Huachang and Bailian area show similar geochemical characteristics with relatively lower contents of C_{19+20}TT, OL and higher contents of unusual tetracyclic terpanes and dino-TAS, which suggests that the related source rocks are composed of mixed organic matter input.

The biomarker distribution of E*ls*$_2$ crude oils from Bailian area display similar characteristics with the E*ls*$_1$ oil samples from Yong'an area, exhibiting strong enrichment in C_{19+20}TT, oleanane and unusual tetracyclic terpanes (Fig. 15). The widespread occurrence of C_{19+20}TT, oleanane and unusual tetracyclic terpanes in the Yong'an and Bailian oils verified the contribution of terrigenous organic matter to their source rocks.

The crude oils in E*ls*$_3$ reservoir can be discriminated from the E*ls*$_2$ and E*ls*$_1$ oils. The E*ls*$_3$ crude oils are characterized by significant abundance of C_{23}TT, but low oleanane, Y_1 and Z_1 contents, indicating a more aquatic organism contribution to the related source rock (Fig. 15). The oil samples from the eastern area have higher dino-TAS contents than the western area, indicating the more dinoflagellates contributions to the related source rocks (Fig. 15). The relevant data was shown in Supplementary Table 2.

5. Discussion

5.1. Depositional environment and biological origin of source rock

Previous studies divided the Liushagang Formation source rocks into E*ls*$_1$, E*ls*$_2$ and E*ls*$_3$ source rocks, and mainly focused on the thermal maturity of different source rocks (Gan et al., 2020). The lack of research on source rock lateral heterogeneity tends to cause the ambiguity of oil origin and the oversimplification of hydrocarbon accumulation model, especially for the complex lacustrine petroleum system. The source rocks were re-divided for further detailed oil-source rock correlations within the sequence and sedimentary framework. The geochemical parameters representing the organic matter source (from algae to terrestrial and algae mixing) could effectively distinguish source rock characteristics difference among E*ls*$_3$ source rock, E*ls*$_1$ and E*ls*$_2$ deltaic source rock, E*ls*$_1$ and E*ls*$_2$ lacustrine source rock.

All samples from the Liushagang Formation show similar Pr/Ph

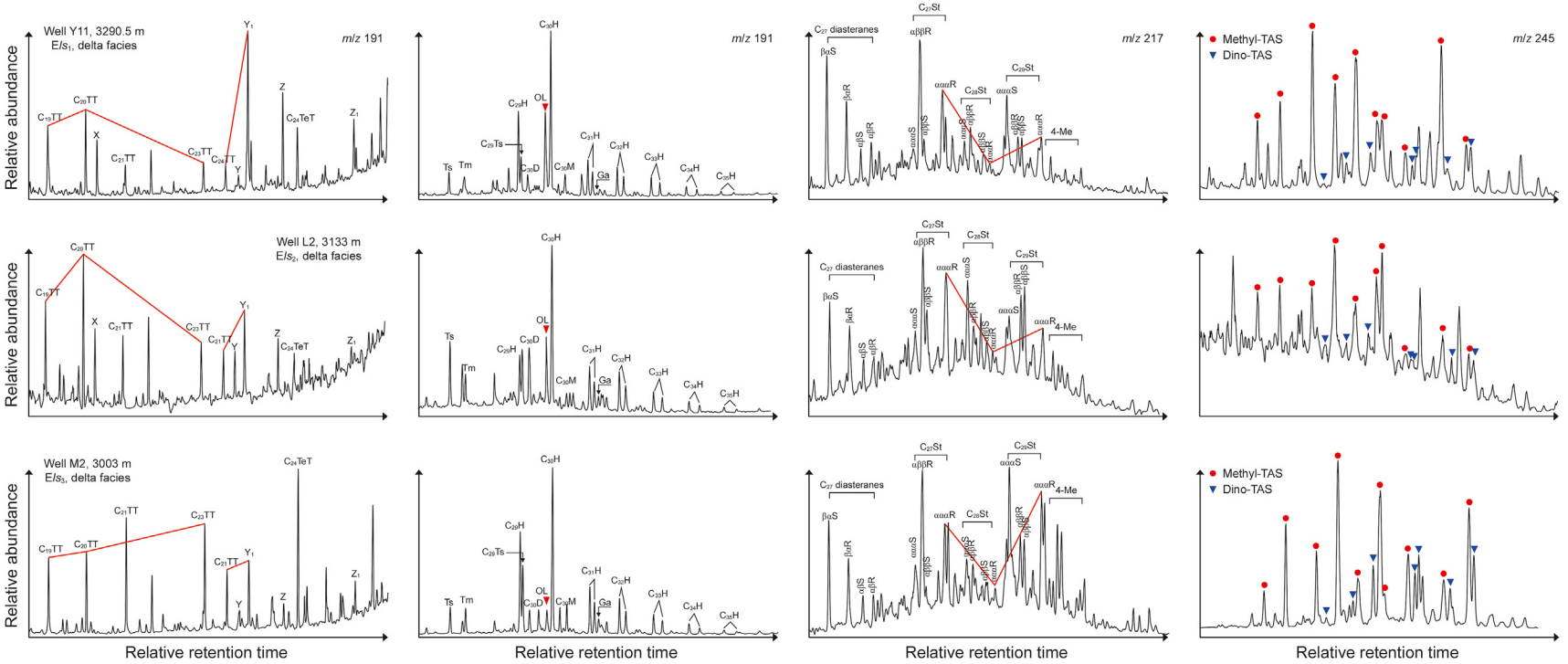

Fig. 10. Mass chromatograms of representative deltaic source rocks in the Fushan Depression, including the saturated hydrocarbons of terpane (*m/z* 191), hopane (*m/z* 191), sterane (*m/z* 217) and aromatic hydrocarbons of triaromatic steroid (*m/z* 245).

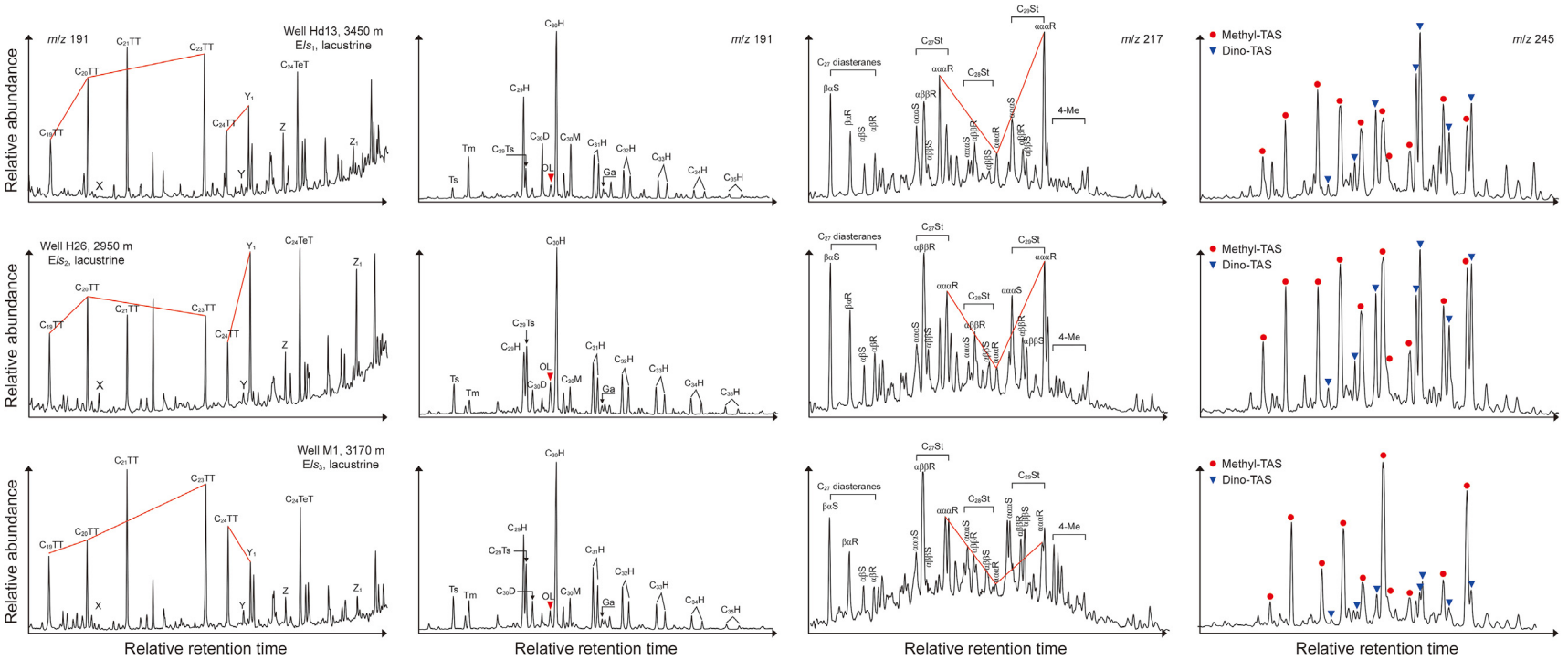

Fig. 11. Mass chromatograms of representative lacustrine source rocks in the Fushan Depression, including the saturated hydrocarbons of terpane (*m/z* 191), hopane (*m/z* 191), sterane (*m/z* 217) and aromatic hydrocarbons of triaromatic steroid (*m/z* 245).

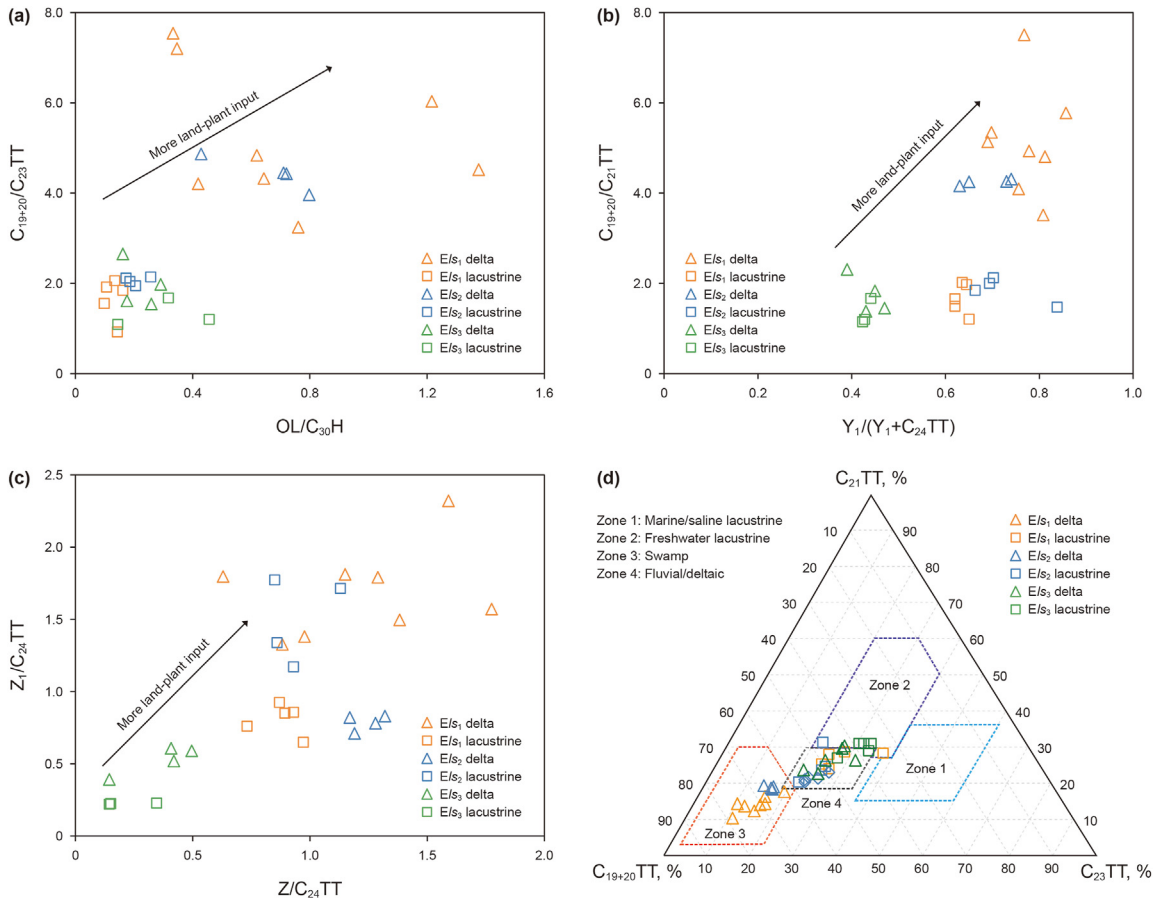

Fig. 12. Cross-plots of selected terpane parameters **(a)**, **(b)** and **(c),** and ternary diagram of C_{19+20}TT, C_{21}TT and C_{23}TT **(d)** (after Xiao et al. (2019c)), showing the organic matter sources and sedimentary conditions of the potential source rocks in Fushan Depression.

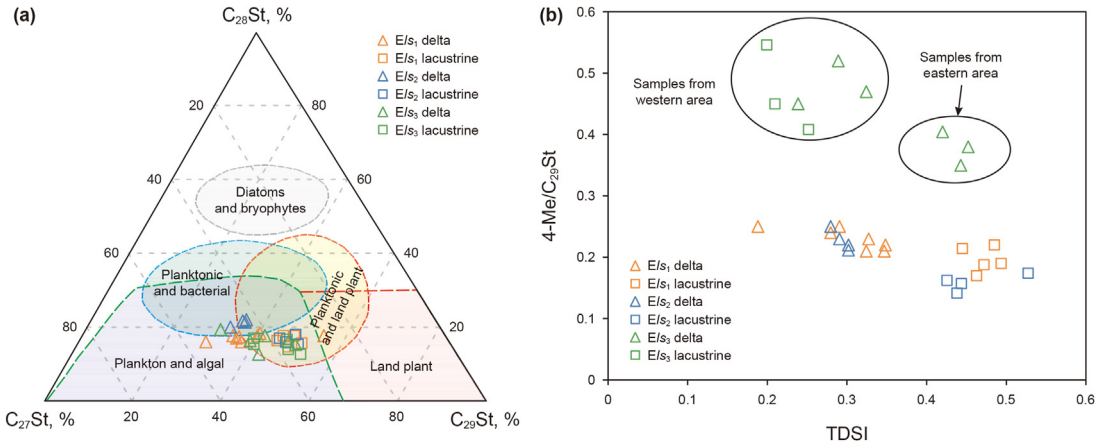

Fig. 13. Ternary diagram of C_{27}–C_{29} sterane **(a)** (after Huang and Meinschein (1979)) and cross-plot of 4-Me/C_{29} St vs. TDSI **(b)**, showing the organic matter sources of the potential source rocks in Fushan Depression.

and Ga/C_{30}H values, indicating an oxidizing and freshwater depositional environment. A comprehensive analysis of biomarker compositions reveals the similarity between the E*ls*$_3$ source rocks from delta and lacustrine facies, which are distinct from the E*ls*$_1$ and E*ls*$_2$ source rocks (Figs. 12 and 13). While the E*ls*$_1$ and E*ls*$_2$ source rocks from diverse sedimentary facies display significant difference on their geochemical characteristics. The E*ls*$_3$ source rocks are characterized by relatively high content of C_{23}TT and C_{30} 4-Me St, corresponding to more contributions of planktonic algae. The E*ls*$_1$ and E*ls*$_2$ deltaic source rocks show the remarkable abundance of C_{19+20}TT and oleanane, indicating the higher proportion of terrigenous plant materials. The E*ls*$_1$ and E*ls*$_2$ lacustrine source rocks contain high abundance of unusual tetracyclic terpane as well as the dino-TAS, but low concentrations of C_{19+20}TT and oleanane, reflecting the mixed contributions of planktonic algae, bacteria and terrigenous plant materials (Figs. 12 and 13).

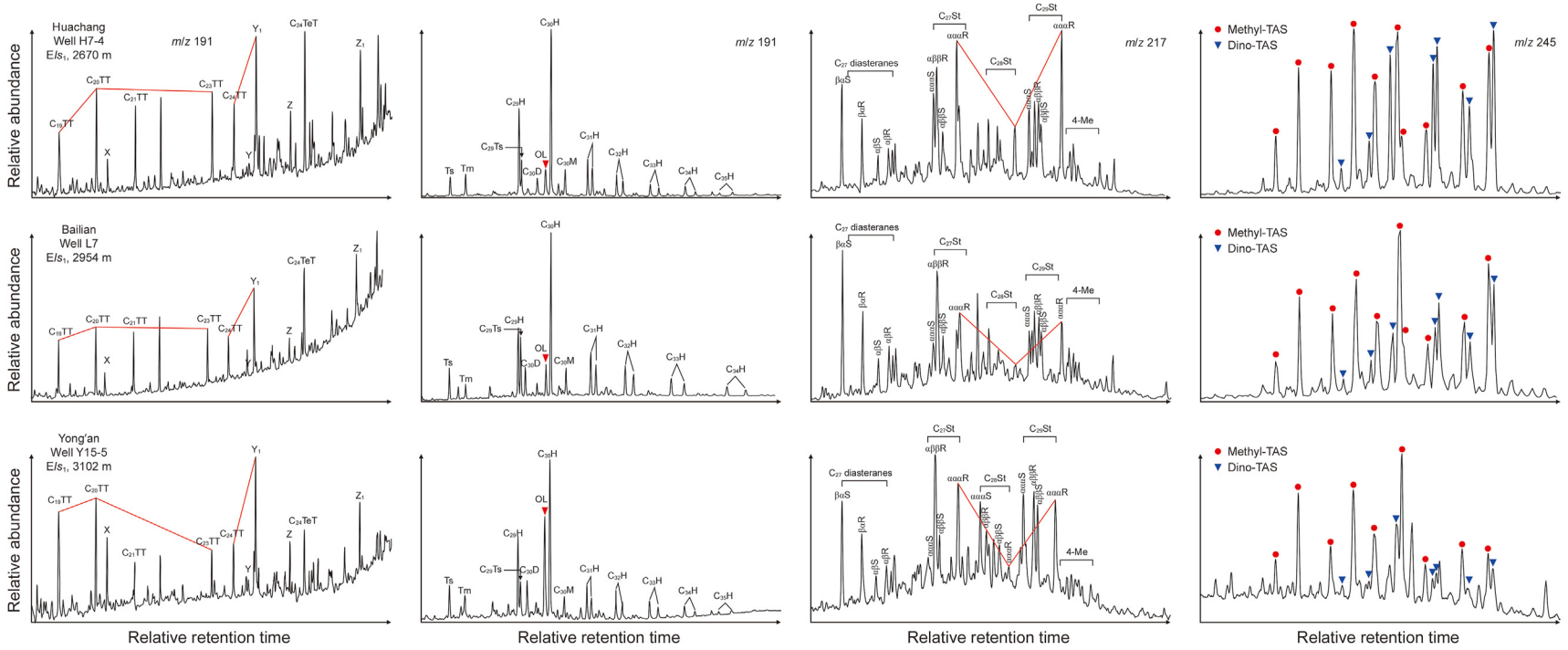

Fig. 14. Mass chromatograms of representative Es_1 crude oils in the Fushan Depression, including the saturated hydrocarbons of terpane (*m/z* 191), hopane (*m/z* 191), sterane (*m/z* 217) and aromatic hydrocarbons of triaromatic steroid (*m/z* 245).

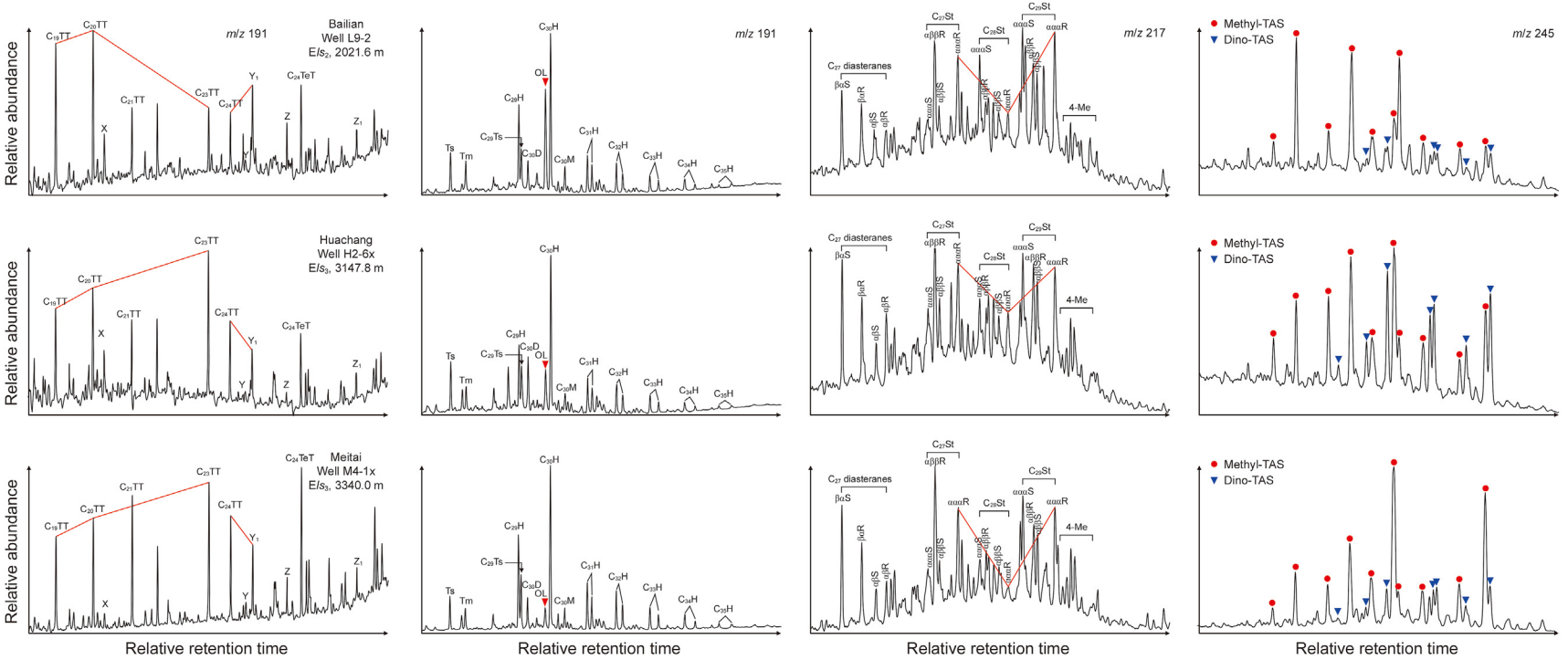

Fig. 15. Mass chromatograms of representative Els_2 and Els_3 crude oils in the Fushan Depression, including the saturated hydrocarbons of terpane (*m/z* 191), hopane (*m/z* 191), sterane (*m/z* 217) and aromatic hydrocarbons of triaromatic steroid (*m/z* 245).

5.2. Maturity of crude oil

The aromatic hydrocarbon maturity parameters have been widely applied in the assessment of crude oil maturity (Chakhmakhchev and Suzuki, 1995). Naphthalene and phenanthrene series are important polycyclic aromatic compounds in crude oils. According to thermodynamic stability theory—β-substituted isomers are more stable than α-substituted isomers—maturity parameters such as methylnaphthalene ratio (MNR), dimethylnaphthalene ratio (DNR), trimethylnaphthalene ratio (TMNr) and tetramethylnaphthalene ratio (TeMNr) were established (Radke et al., 1982; van Aarssen et al., 1999). Phenanthrene Distribution Fraction (MPDF), less influenced by kerogen types or lithology, was thought to be a reliable thermal maturity indicator. MPDF parameters (F1 and F2), proposed by Kvalheim et al. (1987), were calculated by the relative abundance of the four isomers of methylphenanthrene. Calibrations between vitrinite reflectance (Ro) and the MPDF parameters have also been conducted (Bao et al., 1992).

According to cross plots of MPDF parameters (F1 and F2) (Fig. 16(a)), the crude oils in the Els_1 reservoirs are in the mature stage. Crude oils in the Yong'an area exhibit higher maturity compared to those in the Huachang-Bailian area. The maturity parameters of Els_2 and Els_3 crude oil samples change significantly, especially in the eastern (Huachang-Bailian) area (Fig. 16), which may be attribute to the hydrocarbon migration (Li et al., 2018b). Els_2 and Els_3 crude oils from eastern area have relatively higher values of TMNr and TeMNr, indicating higher thermal maturity compared to the Els_3 crude oils from western area (Fig. 16(b)). The eastern oil samples indicated by the F1 and F2 parameters fall within the high-maturity interval, whereas the western oil samples are mature (Fig. 16(a)).

Radke (1988) proposed the methylphenanthrene ratio (MPR) and the relationship between R_o and MPR was established, which is more suitable for the maturity evaluation of lacustrine crude oil (Yang et al., 2018). According to the empirical equation, the calculated equivalent vitrinite reflectance (R_c %) of Els_3 crude oils from western area and Els_1 crude oils from Huachang and Yong'an area is between 0.56% and 0.69%, corresponding to the low-mature to mature stage. While the R_c of Els_2 and Els_3 from eastern area is between 0.69% and 1.35%, indicating the mature to high-mature stage (Supplementary Table 3).

5.3. Oil-oil and oil-source rock correlations

The hierarchical cluster analysis (HCA) was conducted to classify oil groups. A total of 11 geochemical parameters relative to biomarkers are selected for HCA analysis (Supplementary Table 2), which was accomplished by SPSS software. The related parameters are closely related to the biological source and thus are helpful for distinguishing the source rocks and crude oil samples (Xiao et al., 2019c; Wang et al., 2022b; You et al., 2021). The HCA result shows that all crude oil samples can be classified into three groups (Fig. 17).

Group A oils, mainly presented in the Els_1 reservoirs of Huachang-Bailian area, are characterized by relatively high contents of unusual tetracyclic terpane and dino-TAS, suggesting a mixed contribution of terrestrial plants and aquatic organisms to their related source rocks. All these data points of group A oils are closely plotted in one group in each cross plot (Fig. 18(a)–(d)), indicating a high degree of similarity of these oil samples in biomarker composition. They also fall into the zone of Els_1 and Els_2 lacustrine source rocks, suggesting that group A oils are mainly derived from these Els_1 and Els_2 source rocks. The R_c of group A oil is in the range of 0.59%–0.65%, indicating the low-mature to mature stage. The lower part of Els_1 (EST) and the upper part of Els_2 (RST), with thick lacustrine mudstones deposited, have entered the mature stage with high hydrocarbon-generating intensity (Figs. 6 and 19) (Zeng et al., 2023). Two structural layers were divided by the mfs in Els_2, with antithetic fault in the lower structural layer and consequent fault in the upper structural layer. Crude oils migrate vertically along the normal fault to Els_1 reservoirs (Fig. 19) (Gan et al., 2020).

Group B oils, found in Els_1 reservoir of Yong'an area and Els_2 reservoir of Bailian area, were characterized by abundant C_{19+20}TT, oleanane, unusual tetracyclic terpanes but low abundance of C_{30} 4-Me St and dino-TAS (Fig. 18). This type oil probably derived from source rocks with increased contribution of terrigenous organic matter. Group B crude oil could be further subdivided into B1 and B2, which are sourced from delta source rocks in the Els_1 and Els_2, respectively (Figs. 17 and 18). The subgroup B1 and B2 crude oils have slight differences in biomarker composition, but obvious distinction in maturity (Fig. 16). The subgroup B1 oils, distributed in the Els_1 reservoir of the Huangtong Sag, are in low-mature to mature stage (R_c = 0.65%–0.69%), corresponding to the Els_1 source rocks in the Huangtong Sag (Fig. 6). The subgroup B2 crude oils,

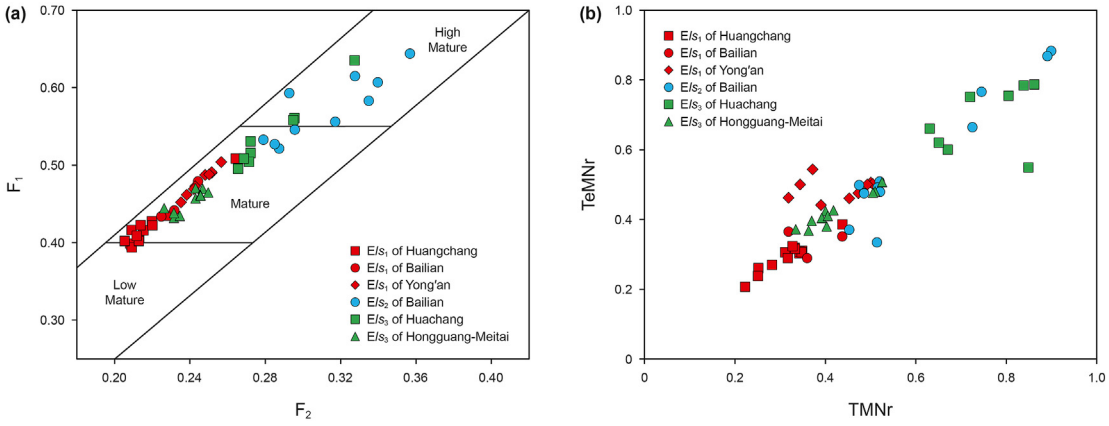

Fig. 16. Cross-plots of **(a)** Methyl-Phenanthrene Distribution Fraction (MPDF) F1 vs F2 (after Kvalheim et al. (1987)) and **(b)** TeMNr vs. TMNr, showing the maturity parameter of crude oils in the Fushan Depression. Note: F1= (2-MP + 3-MP)/(2-MP + 3-MP + 1-MP + 9-MP); F2 = 2-MP/(2-MP + 3-MP + 1-MP + 9-MP); TMNr = 1,3,7-/(1,3,7-+1,2,5-) TMN; TeMNr = 1,3,6,7-/(1,3,6,7-+1,2,5,6-+1,2,3,5-) TeMN.

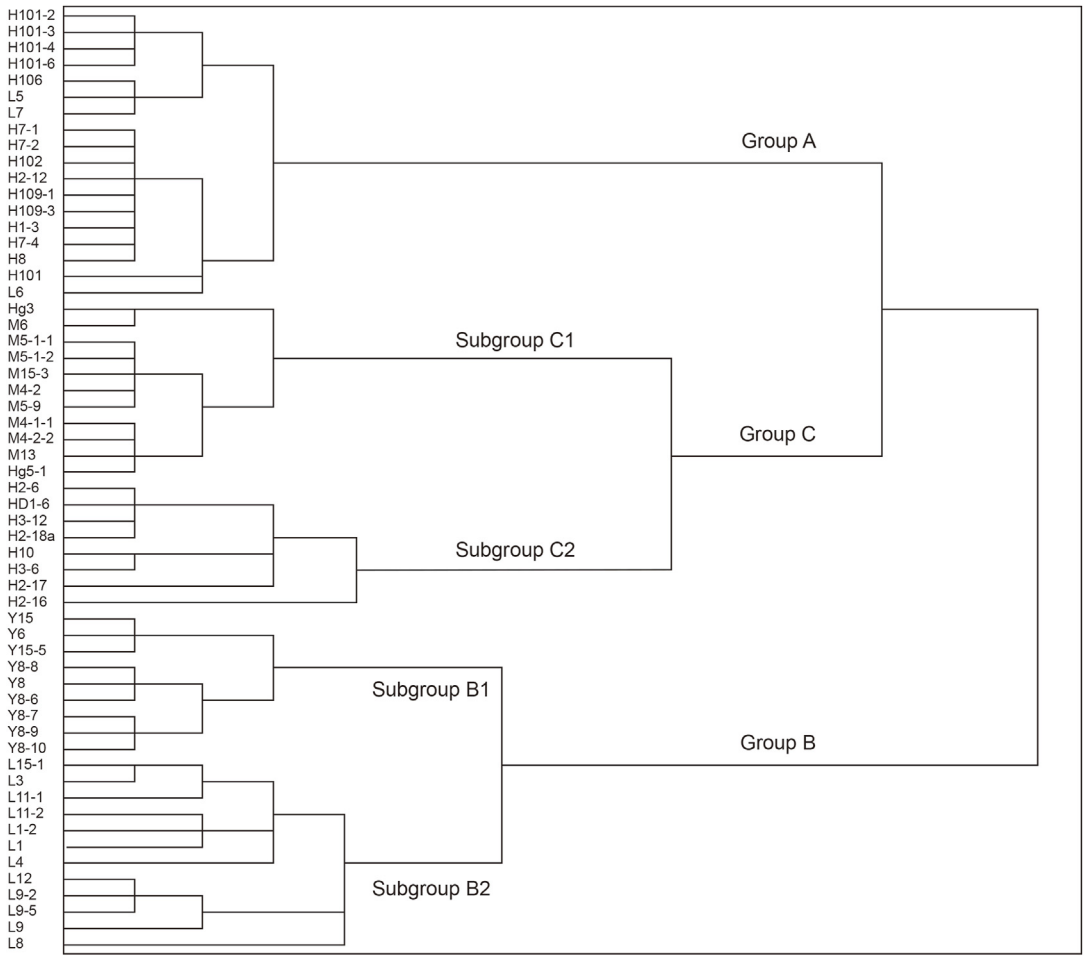

Fig. 17. Dendrogram of hierarchical cluster analysis (HCA) using biomarkers showing oil group classification.

found in the eastern area of the Southern slope zone, have higher maturity with significant variation (R_c = 0.73%–1.23%).

Group C oils are mainly discovered in the Els_3 sandstone reservoirs, which are considered to be originated from the Els_3 source rocks, both deltaic source rocks and lacustrine source rocks. These oils feature low terpenoid biomarker ratios (OL/C_{30}H, C_{19+20}/C_{23}TT, $Y_1/(Y_1+C_{24}TT)$, Z/C_{24}TT, Z_1/C_{24}TT), suggesting less terrestrial plant contribution (Fig. 18). It is noted that the distribution of C_{30} 4-Me St and dino-TAS have slight differences among the Group C oil (Fig. 18(d) and Supplementary Table 2), which can be further subdivided into subgroups C1 and C2 (Figs. 17 and 18). Subgroup C1 oils are collected from most wells in the western area, showing higher C_{30} 4-Me St contents but low dino-TAS concentrations. Whereas the subgroup C2 oils exhibit the opposite pattern, as depicted in Fig. 18(d). The plentiful C_{30} 4-Me St and dino-TAS are associated with contributions from dinoflagellates, while reducing environment is more conducive to the generation of C_{30} 4-Me St (Wang et al., 2008; Chang et al., 2023). The subtle difference between subgroup C1 and C2 oils may be attributed to the sedimentary environments. In addition, the maturity of subgroup C2 oils (R_c = 0.69%–0.88%) is higher than the subgroup C1 oils (R_c = 0.56%–0.66%), which may be related to the high thermal flow caused by volcanic intrusion and the deeper burial depth in the eastern area (Figs. 6 and 19) (Chen et al., 2014; Zeng et al., 2023).

5.4. Implication for petroleum exploration

Three secondary structural units, Huangtong Sag, Bailian Sag and the Southern slope zone, are divided by two secondary faults (Meihua Fault and Lianhua Fault) (Figs. 2 and 19). The Liushagang Formation in the Southern slope zone vertically displays as a double layered structure composed of two sets of fault systems, which were divided by the mfs in Els_2.

The Els_3 reservoirs of Meitai-Hongguang and Huachang-Bailian area are mainly derived from the Els_3 source rocks located in the Southern slope zone due to the missing of Els_3 in the Huangtong Sag and Bailian Sag. The subgroup B2 and group C oils, distributed in the lower tectonic layer, primarily originate from Els_2 deltaic source rocks and Els_3 source rocks, respectively. A series of molecular parameters, such as 4-/1-MDBT, 1-/4-MDBF, were applied to trace oil migration orientations and reservoir filling pathways (Fang et al., 2017; Li et al., 2018b; Wang et al., 2022a). The overall migration orientation of these oils is from north to south, with the sandstone of the braided river delta front served as effective carried beds (Gan et al., 2020). Most sealed faults in the lower tectonic layer are conducive to hydrocarbon accumulation (Gan et al., 2020, 2023). The deeper burial depth and widespread effective source rocks of eastern area, compared to the western area, lead to the high yield in the Huachang Els_3 reservoir.

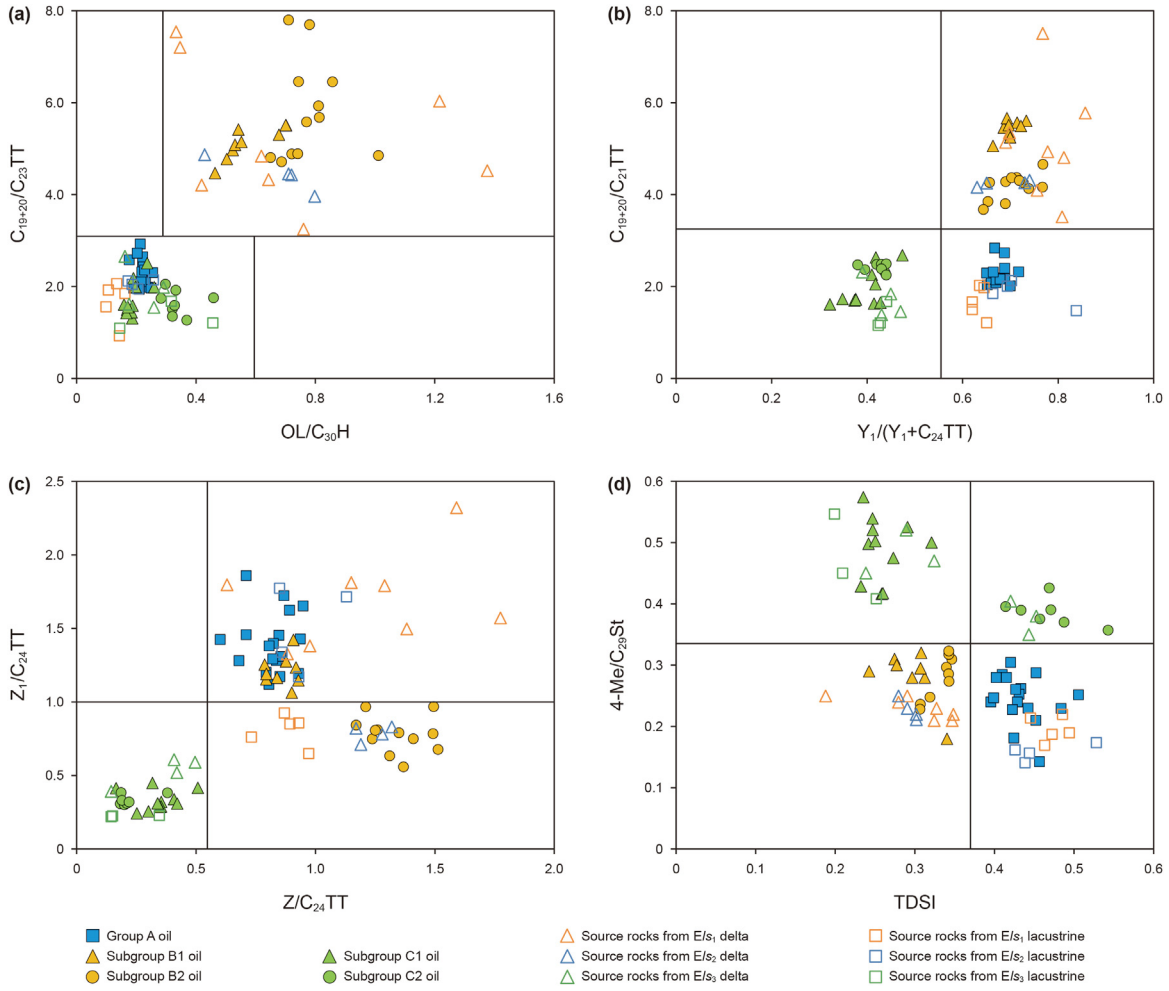

Fig. 18. Cross-plots of selected biomarkers of different oil groups and source rocks for oil-source correlation.

In the upper tectonic layer, the group A oils sourced from Els_1 and Els_2 source rocks migrate vertically along the normal faults and laterally along permeable deltaic sand bodies (Gan et al., 2020, 2023). The high structural position in the Huachang Uplift results in the predominant distribution of group A oils in the Huachang area. In addition, since the low maturity of the Els_2 source rocks in the Western area, no effective Els_1 reservoirs were discovered in the western area (Zeng et al., 2023).

In the Huangtong Sag, the Yong'an area where the delta front sandbodies interacts with deltaic mudstones were mainly developed lithologic traps or structural-lithologic traps in the Els_1. Their restricted distribution may suggest a short-distance migration from the adjacent source rocks. Similarly, the Els_2 of Yong'an area is considered as the favorable exploration area in the future. The Bailian Sag is located in the north of Lianhua Fault, which stratigraphic distribution and structural condition may be similar to the Huangtong Sag. However, findings from the only well drilled in the Bailian Sag indicate poor-quality source rock, rendering it unfavorable for reservoir formation.

Generally, the strong heterogeneity of source rocks controlled by sedimentary facies variations results in the distinct geochemical characteristics of corresponding crude oils. The secondary faults, Meihua Fault and Lianhua Fault, divided the Southern slope zone and the Huangtong Sag into two petroleum systems, causing the differences in hydrocarbon migration and accumulation mechanisms. The range of effective source rocks also have influence on the distribution of reservoir.

6. Conclusion

Source rocks from different sedimentary environments exhibit notable differences in their biomarker composition, especially the organic matter input. Based on the detailed analysis of the biomarker composition, three categories source rocks occurred in the Fushan Depression: Els_3 source rocks (both delta and lacustrine), Els_1 and Els_2 deltaic source rocks, Els_1 and Els_2 lacustrine source rocks. The Els_3 source rocks mainly contributed by aquatic organism. The Els_1 and Els_2 deltaic source rocks are closely related to high terrigenous organic matter input, and the Els_1 and Els_2 lacustrine source rocks are composed of mixed organic matter input.

Three genetic groups of oils (A, B, and C) were recognized on the basis of biomarker composition and hierarchical cluster analysis. The detailed oil-source correlation was conducted within the sequence and sedimentary framework. Group A, B and C oils have good affinity with Els_1 and Els_2 lacustrine source rocks, Els_1 and Els_2 deltaic source rocks, and Els_3 source rocks, respectively. Sedimentary facies have a great influence on the geochemical characteristic of crude oils.

Two petroleum systems were divided by the secondary faults, which result in different hydrocarbon migration and accumulation mechanisms. In the southern slope zone, hydrocarbon mainly

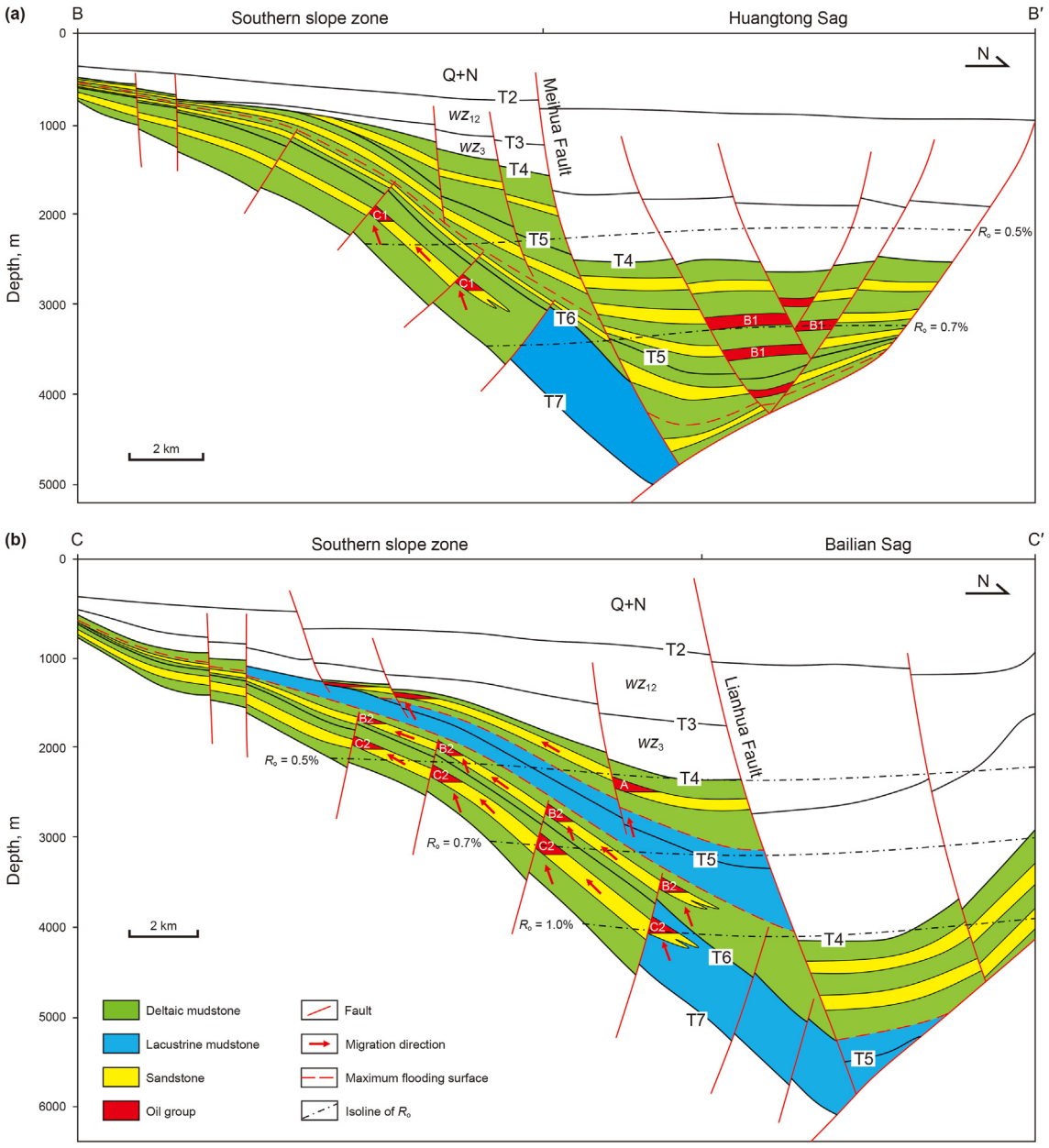

Fig. 19. A conceptual model showing oil migration and distribution patterns in the Huangtong and Bailian sags.

migrated from north to south along the delta front sand body. While in the Huangtong Sag, hydrocarbon display a short-distance migration to the nearby sand body. The Els_2 in the Huangtong Sag has a significant advantage in near-source accumulation, which could be considered as the favorable exploration area in the future.

CRediT authorship contribution statement

Xin Wang: Writing – review & editing, Writing – original draft, Visualization, Investigation, Formal analysis, Data curation, Conceptualization. **Mei-Jun Li:** Visualization, Validation, Supervision, Methodology, Investigation, Formal analysis, Conceptualization. **Yang Shi:** Supervision, Project administration, Funding acquisition, Data curation. **Hao Guo:** Visualization, Validation, Project administration, Funding acquisition. **Bang Zeng:** Validation, Supervision, Data curation, Conceptualization. **Xi He:** Methodology, Investigation, Data curation.

Declaration of competing interest

The authors declare that they have no known competing financial interests or personal relationships that could have appeared to influence the work reported in this paper.

Acknowledgements

This study was funded by the South Oil Exploration and Development Company of PetroChina (2021-HNYJ-010). We would like to thank Shi Shengbao, Zhu Lei, and Zhang Jianfeng of the China University of Petroleum (Beijing) for their assistance and guidance

during the experiment. We also acknowledge three anonymous reviewers for their valuable comments and suggestions, which greatly improve the quality of the manuscript.

Appendix A. Supplementary data

Supplementary data to this article can be found online at https://doi.org/10.1016/j.petsci.2024.08.005.

References

Bao, J.P., Wang, T.G., Zhou, Y.Q., Yu, F.X., Wang, J.J., Zhou, Q.L., Chen, F.J., 1992. The relationship between methyl phenanthrene ratios and the evolution of organic matter. Journal of Jianghan Petroleum Institute 14, 8–19 (in Chinese).

Bohacs, K.M., Carroll, A.R., Neal, J.E., Mankiewicz, P.J., 2000. Lake-basin type, source potential, and hydrocarbon character: an integrated sequence-stratigraphic geochemical framework. AAPG Stud. Geol. 46, 3–34. https://doi.org/10.1306/St46706C1.

Bordenave, M.L., Espitalié, J., Leplat, J.L., Vandenbroucke, M.E., 1993. Screening techniques for source rock evaluation. In: Bordenave, M.L. (Ed.), Applied Petroleum Geochemistry. Editions Technip, Paris, pp. 218–278.

Chang, R., Wang, G.L., Zhang, Z.H., Li, H.Y., Cao, L., Xia, H.Y., 2023. Distribution and genesis of dinoflagellate-derived molecular fossils in Beibuwan Basin. Acta Sedimentol. Sin. 41 (1), 280–288. https://doi.org/10.14027/j.issn.1000-0550.2021.075 (in Chinese).

Chakhmakhchev, A., Suzuki, N., 1995. Saturate biomarkers and aromatic sulfur compounds in oils and condensates from different source rock lithologies of Kazakhstan, Japan and Russia. Org. Geochem. 23 (4), 289–299. https://doi.org/10.1016/0146-6380(95)00018-A.

Chattopadhyay, A., Dutta, S., 2014. Higher plant biomarker signatures of early Eocene sediments of north eastern India. Mar. Petrol. Geol. 57, 51–67. https://doi.org/10.1016/j.marpetgeo.2014.04.004.

Chen, S.B., Gan, H.J., Xia, C.Y., Zhao, Y.D., Wang, G.H., Wang, X., 2014. History simulation of thermal evolution and hydrocarbon generation of source rocks in Bailian sub-Sag, Fushan Sag, Beibuwan Basin. Xinjiang Pet. Geol. 35 (6), 672–677 (in Chinese).

Ekweozor, C., Strausz, O., 1983. Tricyclic terpanes in the Athabasca oil sands: their geochemistry. In: Advances in Organic Geochemistry. Wiley, New York, pp. 746–766.

Er, C., Zhao, J.Z., Wang, R., Wei, Z.K., 2015. Controlling role of sedimentary environment on the distribution of organic-rich shale: a case study of the Chang7 member of the Triassic Yanchang Formation, Ordos Basin. Nat. Gas Geosci. 47, 107–113. https://doi.org/10.11764/j.issn.1672-1926.2015.05.0823 (in Chinese).

Fang, R.H., Li, M.J., Wang, T.G., Liu, X.Q., Yuan, Y., Jiang, W.D., Wang, D.W., Shi, S.B., 2017. Trimethyldibenzothiophenes: molecular tracers for filling pathways in oil reservoir. J. Pet. Sci. Eng. 159, 451–460. https://doi.org/10.1016/j.petrol.2017.09.058.

Fu, J.H., Li, S.X., Xu, L.M., Niu, X.B., 2018. Paleo-sedimentary environmental restoration and its significance of Chang 7 member of triassic yanchang Formation in ordos basin, NW China. Petrol. Explor. Dev. 45, 998–1008. https://doi.org/10.1016/S1876-3804(18)30104-6.

Gan, H.J., Wang, H., Shi, Y., Ma, Q.L., Liu, E.T., Yan, D.T., Pan, Z.J., 2020. Geochemical characteristics and genetic origin of crude oil in the Fushan Sag, Beibuwan Basin, south China sea. Mar. Petrol. Geol. 112, 104114. https://doi.org/10.1016/j.marpetgeo.2019.104114.

Gan, H.J., Gong, S., Tian, H., Wang, H., Chen, J., Ma, Q.L., Liu, K.X., Lu, Z.H., 2023. Geochemical characteristics of inclusion oils and charge history in the Fushan sag, Beibuwan Basin, south China sea. Appl. Geochem. 150, 105598. https://doi.org/10.1016/j.apgeochem.2023.105598.

Hao, F., Zhou, X.H., Zhu, Y.M., Yang, Y.Y., 2011. Lacustrine source rock deposition in response to co-evolution of environments and organisms controlled by tectonic subsidence and climate, Bohai Bay Basin, China. Org. Geochem. 42, 323–339. https://doi.org/10.1016/j.orggeochem.2011.01.010.

Huang, B.J., Xiao, X.M., Cai, D.S., Wilkins, R.W.T., Liu, M.Q., 2011. Oil families and their source rocks in the Weixinan sub-basin, Beibuwan basin, south China sea. Org. Geochem. 42, 134–145. https://doi.org/10.1016/j.orggeochem.2010.12.001.

Huang, B.J., Tian, H., Wilkins, R.W.T., Xiao, X.M., 2013. Geochemical characteristics, palaeoenvironment and formation model of Eocene organic-rich shales in the Beibuwan Basin, South China sea. Mar. Petrol. Geol. 48, 77–89. https://doi.org/10.1016/j.marpetgeo.2013.07.012.

Huang, B.J., Zhu, W.L., Tian, H., Jin, Q.Y., Xiao, X.M., Hu, C.H., 2017. Characterization of Eocene lacustrine source rocks and their oils in the Beibuwan Basin, offshore South China Sea. AAPG Bull. 101 (9), 1395–1423. https://doi.org/10.1306/10171615161.

Huang, W.Y., Meinschein, W.G., 1979. Sterols as ecological indicators. Geochem. Cosmochim. Acta 43, 739–745. https://doi.org/10.1016/0016-7037(79)90257-6.

Hughes, W.B., Holba, A.G., Dzou, L.I.P., 1995. The ratios of dibenzothiophene to phenanthrene and pristane to phytane as indicators of depositional environment and lithology of petroleum source rocks. Geochem. Cosmochim. Acta 59, 3581–3598. https://doi.org/10.1016/0016-7037(95)00225-O.

Kvalheim, O.M., Christy, A.A., Telnaes, N., Bjørseth, A., 1987. Maturity determination of organic matter in coals using the methylphenanthrene distribution. Geochem. Cosmochim. Acta 51, 1883–1888. https://doi.org/10.1016/0016-7037(87)90179-7.

Lai, H.F., Li, M.J., Liu, J.G., Mao, F.J., Xiao, H., He, W.X., Yang, L., 2018. Organic geochemical characteristics and depositional models of Upper Cretaceous marine source rocks in the Termit Basin, Niger. Palaeogeogr. Palaeoclimatol. Palaeoecol. 495, 292–308. https://doi.org/10.1016/j.palaeo.2018.01.024.

Lai, H.F., Li, M.J., Jian, X.L., Wang, L.L., Liu, J.P., Wang, G.Y., Liu, P., Dai, J.H., 2020. An integrated sequence stratigraphic-geochemical investigation of the Jurassic source rocks in the North Yellow Sea Basin, eastern China. AAPG Bull. 104 (10), 2145–2171. https://doi.org/10.1306/05212019072.

Li, M.J., Wang, T.G., Liu, J., Zhang, M.Z., Lu, H., Ma, Q.L., Gao, L.H., 2007. Characteristics of oil and gas accumulation in yong'an-Meitai area of the Fushan depression, Beibuwan Basin, south China sea. Petrol. Sci. 4, 23–33. https://doi.org/10.1007/BF03187452.

Li, M.J., Lai, H.F., Mao, F.J., Liu, J.G., Xiao, H., Tang, Y.J., 2018a. Geochemical assessment of source rock within a stratigraphic geochemical framework: taking Termit Basin (Niger) as an example. Earth Sci. 43 (10), 3603–3615. https://doi.org/10.3799/dqkx.2018.223 (in Chinese).

Li, M.J., Liu, X.Q., Wang, T.G., Jiang, W.D., Fang, R.H., Yang, L., Tang, Y.J., 2018b. Fractionation of dibenzofurans during subsurface petroleum migration: based on molecular dynamics simulation and reservoir geochemistry. Org. Geochem. 115, 220–232. https://doi.org/10.1016/j.orggeochem.2017.10.006.

Li, Y., Lin, S., Wang, H., Luo, D., 2017. Depositional setting analysis using seismic sedimentology: example from the Paleogene Liushagang sequence in the Fushan depression, South China Sea. Geodesy Geodyn 8, 347–355. https://doi.org/10.1016/j.geog.2017.05.001.

Li, Y., Wang, H., Zhu, J.Q., Zhang, G.T., Guo, H., Li, X.H., Lin, S., Min, J., 2022. Depositional evolution and models for a deep-lacustrine gravity flow system in a half-graben rifted sag, Beibuwan Basin, South China Sea. Geol. Acta 20 (20.3), 1–18. https://doi.org/10.1344/GeologicaActa2022.

Liang, C., Cao, Y.C., Liu, K.Y., Jiang, Z.X., Wu, J., Hao, F., 2018. Diagenetic variation at the lamina scale in lacustrine organic-rich shales: implications for hydrocarbon migration and accumulation. Geochem. Cosmochim. Acta 229, 112–128. https://doi.org/10.1016/j.gca.2018.03.017.

Liu, L.J., Tong, Y.M., Ji, Y.L., Kuang, C.W., Lu, M.G., 2003. Sedimentary characteristics and developing background of the sublacustrine fan in the Liushagang formation of the Fushan Depression, the Beibuwan Basin. Pet. Geol. Exp. 25 (2), 110–115. https://doi.org/10.11781/sysydz200302110 (in Chinese).

Liu, E.T., Wang, H., Lin, Z.L., Li, Y., Ma, Q.L., 2012. Characteristics and hydrocarbon enrichment rules of transfer zone in Fushan Sag. Beibuwan Basin. J. Cent. S. Univ. 43 (10), 3946–3953 (in Chinese).

Liu, E.T., Wang, H., Li, Y., Zhou, W., Leonard, N.D., Lin, Z.L., Ma, Q.L., 2014. Sedimentary characteristics and tectonic setting of sublacustrine fans in a half-graben rift depression, Beibuwan Basin, South China Sea. Mar. Petrol. Geol. 52, 9–21. https://doi.org/10.1016/j.marpetgeo.2014.01.008.

Liu, E.T., Wang, H., Li, Y., Leonard, N.D., Feng, Y.X., Pan, S.Q., Xia, C.Y., 2015. Relative role of accommodation zones in controlling stratal architectural variability and facies distribution: insights from the Fushan Depression, South China Sea. Mar. Petrol. Geol. 68, 219–239. https://doi.org/10.1016/j.marpetgeo.2015.08.027.

Liu, E.T., Wang, H., Uysal, I.T., Zhao, J.X., Wang, X.C., Feng, Y.X., Pan, S.Q., 2017. Paleogene igneous intrusion and its effect on thermal maturity of organic-rich mudstones in the Beibuwan Basin, South China Sea. Mar. Petrol. Geol. 86, 733–750. https://doi.org/10.1016/j.marpetgeo.2017.06.026.

Liu, E.T., Uysal, I.T., Wang, H., Feng, Y.X., Pan, S.Q., Yan, D.T., Nguyen, A.D., Zhao, J.X., 2021. Timing and characterization of multiple fluid flow events in the Beibuwan Basin, northern South China Sea: implications for hydrocarbon maturation. Mar. Petrol. Geol. 123, 104754. https://doi.org/10.1016/j.marpetgeo.2020.104754.

Lu, Z.H., Gan, H.J., Shi, Y., Chen, S.B., Wang, H., Ma, Q.L., 2016. Geochemical characteristics of crude oil and oil source correlation in the western Fushan Depression. Earth Sci. 41 (11), 111–122. https://doi.org/10.3799/dqkx.2016.132 (in Chinese).

Lu, J.G., Liao, J.B., Liu, X.J., Li, Y., Yao, J.L., He, Q.B., Xiao, Z.L., He, X., Fu, X.Y., Li, X.M., 2022. Geochemistry of different source rocks and oil-source correlation of lacustrine sedimentary successions: a case study of the Triassic Yanchang formation in the Dingbian-Wuqi Area, Ordos Basin, Northern China. J. Asian Earth Sci. 232, 105216. https://doi.org/10.1016/j.jseaes.2022.105216.

Ma, Q.L., Zhao, S.E., Liao, Y.T., Lin, Z.L., 2012. Sequence architectures of paleogene Liushagang Formation and its significance in fushan sag of the Beibuwan Basin. Earth Sci. J. China Univ. Geosci. 37 (4), 667–678. https://doi.org/10.3799/dqkx.2012.076 (in Chinese).

Moldowan, J.M., Seifert, W.K., Gallegos, E.J., 1985. Relationship between petroleum composition and depositional environment of petroleum source rock. AAPG Bull. 69, 1255–1268. https://doi.org/10.1080/10916469808949779.

Mukhopadhyay, P.K., Wade, J.A., Kruge, M.A., 1995. Organic facies and maturation of Jurassic/Cretaceous rocks, and possible oil-source rock correlation based on pyrolysis of asphaltenes, Scotian Basin, Canada. Org. Geochem. 22, 85–104. https://doi.org/10.1016/0146-6380(95)90010-1.

Peters, K.E., Walters, C.C., Moldowan, J.M., 2005. The Biomarker Guide: Biomarkers and Isotopes in Petroleum Exploration and Earth History, second ed. vol 2. Cambridge University Press, Cambridge.

Peters, K.E., Snedden, J.W., Sulaeman, A., Sarg, J.F., Enrico, R.J., 2000. A new geochemical-sequence stratigraphic model for the mahakam delta and makassar slope, Kalimantan, Indonesia. AAPG Bull. 84 (1), 12–44. https://doi.org/10.1306/C9EBCD51-1735-11D7-8645000102C1865D.

Radke, M., Welte, D.H., Willsch, H., 1982. Geochemical study on a well in the Western Canada Basin: relation of the aromatic distribution pattern to maturity of organic matter. Geochem. Cosmochim. Acta 46, 1–10. https://doi.org/10.1016/0016-7037(82)90285-X.

Radke, M., 1988. Application of aromatic compounds as maturity indicators in source rocks and crude oils. Mar. Petrol. Geol. 5 (3), 224–236. https://doi.org/10.1016/0264-8172(88)90003-7.

Robison, C.R., Smith, M.A., Royle, R.A., 1999. Organic facies in Cretaceous and Jurassic hydrocarbon source rocks, Southern Indus basin, Pakistan. Int. J. Coal Geol. 39, 205–225. https://doi.org/10.1016/S0166-5162(98)00046-9.

Samuel, O.J., Kildahl-Andersen, G., Nytoft, H.P., Johansen, J.E., Jones, M., 2010. Novel tricyclic and tetracyclic terpanes in Tertiary deltaic oils: structural identification, origin and application to petroleum correlation. Org. Geochem. 41, 1326–1337. https://doi.org/10.1016/j.orggeochem.2010.10.002.

Schwangler, M., Harris, N.B., Waldron, J.W.F., 2020. Source rock characterization and oil-to-source rock correlation of a Cambrian -Ordovician fold-and-thrust belt petroleum system, western Newfoundland. Mar. Petrol. Geol. 115, 104283. https://doi.org/10.1016/j.marpetgeo.2020.104283.

Shanmugam, G., 1985. Significance of coniferous rain forests and related organic matter in generating commercial quantities of oil, Gippsland basin, Australia. AAPG Bull. 69, 1241–1254. https://doi.org/10.1306/AD462BC3-16F7-11D7-8645000102C1865D.

Sinninghe Damsté, J.S., Kenig, F., Koopmans, M.P., Koster, J., Schouten, S., Hayes, J.M., de Leeuw, J.W., 1995. Evidence for gammacerane as an indicator of water column stratification. Geochem. Cosmochim. Acta 59, 1895–1900. https://doi.org/10.1016/0016-7037(95)00073-9.

SY/T 5735-2019, 2019. Geochemical method for source rock evaluation. China's National Energy Administration: Beijing, China.

Tao, S.Z., Wang, C.Y., Du, J.G., Liu, L., Chen, Z., 2015. Geochemical application of tricyclic and tetracyclic terpanes biomarkers in crude oils of NW China. Mar. Petrol. Geol. 67 (6), 460–467. https://doi.org/10.1016/j.marpetgeo.2015.05.030.

van Aarssen, B.G., Bastow, T.P., Alexander, R., Kagi, R.I., 1999. Distributions of methylated naphthalenes in crude oils: indicators of maturity, biodegradation and mixing. Org. Geochem. 30, 1213–1227. https://doi.org/10.1016/S0146-6380(99)00097-2.

Volkman, J.K., Kearney, P., Jeffrey, S.W., 1990. A new source of 4-methyl sterols and 5α (H)-stanols in sediments: prymnesiophyte microalgae of the genus Pavlova. Org. Geochem. 15, 489–497. https://doi.org/10.1016/0146-6380(90)90094-G.

Wang, G.L., Wang, T.G., Simoneit, B.R.T., Chen, Z.L., Zhang, L.Y., Xu, J.L., 2008. The distribution of molecular fossils derived from dinoflagellates in Paleogene lacustrine sediments (Bohai Bay Basin, China). Org. Geochem. 39 (11), 1512–1521. https://doi.org/10.1016/j.orggeochem.2008.07.013.

Wang, G.H., Huang, C.Y., Liu, E.T., Li, Y., Pan, S.Q., 2014. Characteristics of slope-breaks and its control on sedimentation and hydrocarbon accumulation of Liushagang Formation in gentle slope of south Fushan sag. J. Cent. South Univ. (Sci. Technol.) 45 (5), 1531–1542. https://doi.org/10.1021/la502813n (in Chinese).

Wang, G.H., Wang, H., Gan, H.J., Shi, Y., Zhao, Y.D., Chen, S.B., 2016. Oil source and migration process in oblique transfer zone of Fushan Sag, northern South China Sea. J. Cent. South Univ. 23 (3), 654–668. https://doi.org/10.1007/s11771-016-3111-3.

Wang, X., Lu, Z.H., Li, M.J., Guo, H., Zhu, Z.L., Li, X.H., Yang, C.Y., Zeng, B., Wang, F.Z., Ran, Z.C., 2022a. Petroleum charging history of the paleogene sandstone reservoirs in the Huangtong sag of the fushan depression, south China sea. Energies 15 (4), 1374. https://doi.org/10.3390/en15041374.

Wang, N., Xu, Y.H., Wang, F.L., Liu, Y., Huang, Q., Huang, X., 2022b. Identification and geochemical significance of unusual C24 tetracyclic terpanes in Shahejie Formation source rocks in the Bozhong subbasin, Bohai Bay Basin. Petrol. Sci. 19 (5), 1993–2003. https://doi.org/10.1016/j.petsci.2022.03.025.

Wolff, G.A., Lamb, N.A., Maxwell, J.R., 1986. The origin and fate of 4-methyl steroid hydrocarbons. I. Diagenesis of 4-methyl sterenes. Geochem. Cosmochim. Acta 50, 335–342. https://doi.org/10.1016/0016-7037(86)90187-0.

Xiao, H., Wang, T.G., Li, M.J., Fu, J., Tang, Y.J., Shi, S.B., Yang, Z., Lu, X.L., 2018. Occurrence and distribution of unusual tri- and tetracyclic terpanes and their geochemical significance in some paleogene oils from China. Energy Fuels 32 (7), 7393–7403. https://doi.org/10.1021/acs.energyfuels.8b01025.

Xiao, H., Wang, T.G., Li, M.J., Lai, H.F., Liu, J.G., Mao, F.J., Tang, Y.J., 2019a. Geochemical characteristics of Cretaceous Yogou Formation source rocks and oil-source correlation within a sequence stratigraphic framework in the Termit Basin, Niger. J. Pet. Sci. Eng. 172, 360–372. https://doi.org/10.1016/j.petrol.2018.09.082.

Xiao, H., Li, M.J., Liu, J.G., Mao, F.J., Cheng, D.S., Yang, Z., 2019b. Oil-oil and oil-source rock correlations in the Muglad Basin, Sudan and South Sudan: new insights from molecular markers analyses. Mar. Petrol. Geol. 103, 351–365. https://doi.org/10.1016/j.marpetgeo.2019.03.004.

Xiao, H., Li, M.J., Yang, Z., Zhu, Z.L., 2019c. Distribution patterns and geochemical implications of C19–C23 tricyclic terpanes in source rocks and crude oils occurring in various depositional environments. Geochimica 49, 161–170. https://doi.org/10.19700/j.0379-1726.2019.02.006 (in Chinese).

Xiao, H., Li, M.J., Nettersheim, B.J., 2024. Short chain tricyclic terpanes as organic proxies for paleo-depositional conditions. Chem. Geol. 652, 122023. https://doi.org/10.1016/j.chemgeo.2024.122023.

Yang, L., Li, M.J., Wang, T.G., Shi, Y., 2016. Dibenzothiophenes and benzonaphthothiophenes in oils, and their application in identifying oil filling pathways in Eocene lacustrine clastic reservoirs in the Beibuwan Basin, South China Sea. J. Pet. Sci. Eng. 146, 1026–1036. https://doi.org/10.1016/j.petrol.2016.07.004.

Yang, S.B., Lai, H.F., Li, M.J., Yang, L., Wang, H., 2018. The relationship between methylphenanthrene index, methylphenanthrene ratio and maturity in lacustrine source rocks. J. Yangtze Univ.: J. Nat. Resour. Life Sci. Educ. 15 (19), 12–17. https://doi.org/10.16772/j.cnki.1673-1409.2018.19.003 (in Chinese).

You, B., Ni, Z.Y., Chen, J.F., Wang, G.L., Xiao, H., Wang, Y.S., Song, G.Q., 2021. A distinct oil group in the Dongying Depression, Bohai Bay Basin, China: new insights from norcholestane and triaromatic steroid analyses. Org. Geochem. 162, 104316. https://doi.org/10.1016/j.orggeochem.2021.104316.

Yuan, W., Liu, G.D., Zhou, X.X., Bulseco, A., 2022. Linking hydrothermal activity with organic matter accumulation in the Chang 7 black shale of Yanchang Formation, Ordos Basin, China. Fronti. Earth Sci. 10, 786634. https://doi.org/10.3389/feart.2022.786634.

Zeng, B., Li, M.J., Wang, N., Shi, Y., Wang, F.Z., Wang, X., 2022. Geochemistry and heterogeneous accumulation of organic matter in lacustrine basins: a case study of the Eocene Liushagang Formation in the Fushan Depression, South China Sea. Petrol. Sci. 19 (6), 2533–2548. https://doi.org/10.1016/j.petsci.2022.07.008.

Zeng, B., Lu, Z.H., Yang, T.T., Shi, Y., Guo, H., Wang, X., Liao, F.Y., Li, M.J., 2023. Hydrocarbon generation history of the Eocene source rocks in the Fushan Depression, South China Sea: insights from a basin modeling study. Processes 11, 2051. https://doi.org/10.3390/pr11072051.

Zhang, S.C., Huang, H.P., 2005. Geochemistry of Palaeozoic marine petroleum from the Tarim Basin, NW China: Part 1. Oil family classification. Org. Geochem. 36 (8), 1204–1214. https://doi.org/10.1016/j.orggeochem.2005.01.013.

Zhang, M.Z., Ji, L.M., Wu, Y.D., He, C., 2015. Palynofacies and geochemical analysis of the Triassic Yanchang Formation, Ordos Basin: implications for hydrocarbon generation potential and the paleoenvironment of continental source rocks. Int. J. Coal Geol. 152, 159–176. https://doi.org/10.1016/j.coal.2015.11.005.

Zhao, J.H., Jin, Z.J., Jin, Z.K., Geng, Y.K., Wen, X., Yan, C.N., 2016. Applying sedimentary geochemical proxies for paleoenvironment interpretation of organic-rich shale deposition in the Sichuan Basin, China. Int. J. Coal Geol. 163, 52–71. https://doi.org/10.1016/j.coal.2016.06.015.

Zhu, C.Z., Gang, W.Z., Zhao, X.Z., Chen, G., Pei, L.X., Wang, Y.F., Yang, S.R., Pu, X.G., 2022. Reconstruction of oil charging history in the multi-source petroleum system of the Beidagang buried-hill structural belt in the Qikou Sag, Bohai Bay Basin, China: based on the integrated analysis of oil-source rock correlations, fluid inclusions and geologic data. J. Pet. Sci. Eng. 208, 109197. https://doi.org/10.1016/j.petrol.2021.109197.